

**ISTANBUL TECHNICAL UNIVERSITY ★ GRADUATE SCHOOL OF SCIENCE**  
**ENGINEERING AND TECHNOLOGY**

**INVESTIGATION OF THE EFFECT OF ELECTROSPINNING PARAMETERS  
ON POLYURETHANE NANOFIBER DIAMETER AND FIBER  
MORPHOLOGY**

**M.Sc. THESIS**

**Sassan JAHANGIRI**

**Department of Textile Engineering**

**Thesis Advisor: Prof. Dr. Hale KARAKAS**

**May 2013**



**ISTANBUL TECHNICAL UNIVERSITY ★ GRADUATE SCHOOL OF SCIENCE**  
**ENGINEERING AND TECHNOLOGY**

**INVESTIGATION OF THE EFFECT OF ELECTROSPINNING PARAMETERS  
ON POLYURETHANE NANOFIBER DIAMETER AND FIBER  
MORPHOLOGY**

**M.Sc. THESIS**

**Sassan JAHANGIRI  
(503091823)**

**Department of Textile Engineering**

**Textile Engineering Programme**

**Thesis Advisor: Prof. Dr. Hale KARAKAS**

**MAY 2013**



**İSTANBUL TEKNİK ÜNİVERSİTESİ ★ FEN BİLİMLERİ ENSTİTÜSÜ**

**ELEKTRO LİF ÇEKİM PARAMETRELERİNİN POLİÜRETAN NANOLİF  
ÇAPI VE LİF MORFOLOJİSİ ÜZERİNE ETKİSİNİN İNCELENMESİ**

**YÜKSEK LİSANS TEZİ**

**Sassan JAHANGIRI  
(503091823)**

**Tekstil Mühendisliği**

**Tekstil Mühendisliği Programı**

**Tez Danışmanı: Prof. Dr. Hale KARAKAŞ**

**MAYIS 2013**



**Thesis Advisor : Prof. Dr. Hale KARAKAS** .....

**Prof. Dr. Fatma Kalaoglu** .....  
Istanbul Technical University

**Date of Defense : 06 June 2013**





*To my beloved parents,*



## **FOREWORD**

Throughout the process of writing my thesis, I obtained much help and encouragement from my supervisor Prof. Dr. Hale KARAKAS. I benefited a great deal from her, great attainment, and patient guidance. I wish to take this opportunity to express my sincere gratitude to her. Also, I heartily thank all the Turkish people in Istanbul for their hospitality and support which accompanied me when I studied as a postgraduate. Besides, I am grateful to my friends and colleagues for their kind concern and great encouragement to me.

Finally, I am indebted to my parents, who rendered me much help and great support, which made it possible for me to finish this thesis on time.

May 2013

Sassan JAHANGIRI  
(Textile Engineer)



## TABLE OF CONTENTS

	<u>Page</u>
<b>FOREWORD.....</b>	<b>ix</b>
<b>TABLE OF CONTENTS .....</b>	<b>xi</b>
<b>ABBREVIATIONS .....</b>	<b>xiii</b>
<b>LIST OF TABLES .....</b>	<b>xv</b>
<b>LIST OF FIGURES .....</b>	<b>xvii</b>
<b>SUMMARY .....</b>	<b>xix</b>
<b>ÖZET .....</b>	<b>xxi</b>
<b>1. INTRODUCTION.....</b>	<b>1</b>
1.1 Purpose of Thesis .....	3
<b>2. LITERATURE REVIEW .....</b>	<b>5</b>
2.1 Electrospinning and the Process Description: .....	5
2.2 Electrospinning Applications .....	9
2.3 Electrospinning Process Parameters.....	11
2.4 PU (polyurethane) Nanofibers Obtained by Electrospinning.....	15
2.5 Characterization of Nanofibers.....	18
2.6 Predictions .....	20
<b>3. EXPERIMENTAL WORK.....</b>	<b>21</b>
3.1 Materials and Chemicals .....	21
3.2 Application Data.....	23
3.3 Utilized Scanning Electron Microscope's Characterizations .....	23
3.4 Preparation of the Nanofibers with Electrospinning Method.....	25
<b>4. CONCLUSIONS AND RECOMMENDATIONS.....</b>	<b>46</b>
4.1 Results and Conclusions.....	46
<b>REFERENCES.....</b>	<b>48</b>
<b>CURRICULUM VITAE.....</b>	<b>53</b>



## **ABBREVIATIONS**

<b>AIC</b>	: Akaike Information Criteria
<b>ANN</b>	: Artificial Neural Network
<b>App</b>	: Appendix
<b>BP</b>	: Backpropagation
<b>CGI</b>	: Common Gateway Interface
<b>ESS</b>	: Error Sum-of-Squares
<b>GARCH</b>	: Generalized Autoregressive Conditional Heteroskedasticity
<b>GIS</b>	: Geographic Information Systems
<b>HCA</b>	: HierarchicalCluster Analysis
<b>Mbps</b>	: Megabits per Second
<b>St</b>	: Station
<b>SWAT</b>	: Soil and Water Assessment Tool
<b>UMN</b>	: University of Minnesota





## LIST OF TABLES

	<b><u>Page</u></b>
<b>Table 3.1 :</b> The technical specifications of the PU polymer used in the study. ....	22
<b>Table 3.2 :</b> LARICOL Solubility/Viscosity in Various Solvents Related to MEK ...	22
<b>Table 3.3 :</b> Physical and Chemical Properties of Utilized PU .....	23
<b>Table 3.4 :</b> Table of prepared samples .....	26



## LIST OF FIGURES

	<u>Page</u>
<b>Figure 2.1</b> : Electrospinning setup .....	7
<b>Figure 2.2</b> : Schematic diagram of a coaxial electrospinning apparatus.....	9
<b>Figure 2.3</b> : Electrospun Fibers Applications .....	10
<b>Figure 2.4</b> : Electrospinning flow between different zones .....	13
<b>Figure 2.5</b> : Effects of process parameters on fiber diameter .....	14
<b>Figure 2.6</b> : step-growth polymerization of Polyurethane. ....	15
<b>Figure 2.7</b> : SEM (Scanning Electron Microscope) .....	18
<b>Figure 3.1</b> : A Set of an Electrospinning Machine.....	21
<b>Figure 3.2</b> : Utilized Scanning Electro Spinning (SEM) Instrument.....	24
<b>Figure 3.3</b> : SEM photo and diameters of nanofibers obtained by 10wt%pu , 45wt% THF , 45wt% DMF.....	25
<b>Figure 3.4</b> : Chart of nanofibers obtained by 10wt% PU , 45wt% THF , 45wt% DMF.....	26
<b>Figure 3.5</b> : 4wt% PU, 15cm nozzle-collector distance, 15KV applied voltage, 0.5 ml/hr polymer flow rate .....	27
<b>Figure 3.6</b> : 4wt% PU, 15cm nozzle-collector distance, 15KV applied voltage, 0.5 ml/hr polymer flow rate .....	28
<b>Figure 3.7</b> : 6wt% PU, 15cm distance, 15kv applied, 0.5ml/hr flow rate.....	29
<b>Figure 3.8</b> : 6wt% PU, 15cm nozzle-collector distance, 15KV applied voltage, 0.5 ml/hr polymer flow rate .....	29
<b>Figure 3.9</b> : SEM micrograph of Sample 3 (7wt% PU, 15kV, 15cm distance, 0.5ml/hr flow rate).....	30
<b>Figure 3.10</b> : Fiber diameter distribution of Sample 3 (7wt% PU, 15 kV, 15 cm distance, 0.5ml/hr flow rate).....	30
<b>Figure 3.11</b> : SEM micrograph of Sample 4 (8wt% PU, 15 kV, 15 cm distance, 0.5ml/hr flow rate).....	31
<b>Figure 3.12</b> : Fiber diameter distribution of Sample 4 (8wt% PU, 15 kV, 15 cm distance, 0.5ml/hr flow rate) .....	31
<b>Figure 3.13</b> : SEM Micrograph Of Sample 5 (9wt% PU, 15 Kv, 15 Cm Distance, 0.5ml/Hr Flow Rate).....	32
<b>Figure 3.14</b> : Fiber diameter distribution of Sample 5 (9wt% PU, 15 kV, 15 cm distance, 0.5ml/hr flow rate) .....	32
<b>Figure 3.15</b> : SEM micrograph of Sample 6 (10wt% PU, 15 kV, 15 cm distance, 0.5ml/hr flow rate) .....	33
<b>Figure 3.16</b> : Fiber diameter distribution of Sample 6 (10wt% PU, 15 kV, 15 cm distance, 0.5ml/hr flow rate) .....	34
<b>Figure 3.17</b> : SEM micrograph of Sample 7 (12wt% PU, 15 kV, 15 cm distance, 0.5ml/hr flow rate) .....	34

<b>Figure 3.18</b> : Fiber diameter distribution of Sample 7 (12wt% PU, 15 kV, 15 cm distance, 0.5ml/hr flow rate) .....	35
<b>Figure 3.19</b> : Nozzle-Collector Distance .....	35
<b>Figure 3.20</b> : SEM micrographs of sample 8 (10cm nozzle-collector distance, 15kv supplied voltage, 10wt% solution concentration, 0.5ml/hr flow rate) .	36
<b>Figure 3.21</b> : Fiber diameter distribution of sample 8 (10cm distance, 15kv supplied voltage, 10wt% solution concentration, 0.5ml/hr flow rate) .....	36
<b>Figure 3.22</b> : SEM micrographs of sample 9 (12.5cm nozzle-collector distance, 15kv supplied voltage, 10wt% solution concentration, 0.5ml/hr flow rate) ..	37
<b>Figure 3.23</b> : Fiber diameter distribution of sample 9 (12.5cm distance, 15kv supplied voltage, 10wt% solution concentration, 0.5ml/hr flow rate) ..	37
<b>Figure 3.24</b> : SEM micrographs of sample 10 (15cm nozzle-collector distance, 15kv supplied voltage, 10wt% solution concentration, 0.5ml/hr flow rate) .	38
<b>Figure 3.25</b> : Fiber diameter distribution of sample 10 (15cm distance, 15kv supplied voltage, 10wt% solution concentration, 0.5ml/hr flow rate) ..	38
<b>Figure 3.26</b> : SEM micrographs of sample 11 (17.5cm nozzle-collector distance, 15kv supplied voltage, 10wt% solution concentration, 0.5ml/hr flow rate) .....	39
<b>Figure 3.27</b> : Fiber diameter distribution of sample 11 (17.5cm distance, 15kv supplied voltage, 10wt% solution concentration, 0.5ml/hr flow rate) ..	39
<b>Figure 3.28</b> : SEM micrographs of sample 12 (20cm nozzle-collector distance, 15kv supplied voltage, 10wt% solution concentration, 0.5ml/hr flow rate) ..	40
<b>Figure 3.29</b> : Fiber diameter distribution of sample 12 (20cm distance, 15kv supplied voltage, 10wt% solution concentration, 0.5ml/hr flow rate) ..	40
<b>Figure 3.30</b> : Utilized DC High Electrical Voltage Supplier .....	41
<b>Figure 3.31</b> : Sample 13, 10kv applied, 10wt% PU, 15cm distance, 0.5ml/hr flow rate .....	42
<b>Figure 3.32</b> : Sample 13, 10kv applied, 10wt% PU, 15cm distance, 0.5ml/hr flow rate.....	42
<b>Figure 3.33</b> : Sample 14, 15kv applied, 10wt% PU, 15cm distance, 0.5ml/hr flow rate .....	43
<b>Figure 3.34</b> : Sample 14, 15kv applied, 10wt% PU, 15cm distance, 0.5ml/hr flow rate.....	43
<b>Figure 3.35</b> : Sample 15, 20kv applied, 10wt% PU, 15cm distance, 0.5ml/hr flow rate .....	44
<b>Figure 3.36</b> : Sample 15, 20kv applied, 10wt% PU, 15cm distance, 0.5ml/hr flow rate.....	44

# **INVESTIGATION OF THE EFFECT OF ELECTROSPINNING PARAMETERS ON POLYURETHANE NANOFIBER DIAMETER AND FIBER MORPHOLOGY**

## **SUMMARY**

High electrostatic fields have wide applications in many industries [J. Cross, 1987]. High electrostatic field can be applied to polymer solution or its melt to produce ultrafine fibers, having diameters in the range of a few nanometers to sub-micrometers, such a technique is called electrostatic spinning or electrospinning.

Due to the exceptionally high surface area to mass ratio of these fibers and the high density of pores on the sub-micrometer length scale of the non-woven webs obtained, electrospinning has a wide range of applications in the industry sector, such as, air and liquid filters, wound dressings, tissue engineering, surface modifications, sound absorptive materials and industrial, medical and hygienic filtrations [Kristine Graham, 2002], [Z. M. Huang, et al, 2003].

Electrospinning parameters, such as, solution concentration, nozzle-collector distance, applied voltage and solution flow rate, directly effect on the morphological appearance and diameters of electro-spun fibers. The purpose of this thesis was to determine the effects of these parameters on the morphology of the nanofibers produced from the utilized specific polymer, which was thermoplastic polyurethane and to determine the optimal amount of these parameters among the tested samples.

The effects of solution conditions on the morphological appearance and the averagediameter of electro-spun fibers were investigated by scanning electron microscopy (SEM) technique. It was observed that the electrospinning properties (i.e. solution concentration, nozzle-collector distance, applied voltage and the solution flow rate) were important factors in the final fiber diameter and fiber morphology. Among these properties, solution concentration was found to have the strongest and the solution flow rate to have the weakest effect.

To investigate the effect of parameters on the morphology of the fibers, samples with the same parameters were made in a way that in each sample, one of the parameters was variable and all the other ones were remained constant. For instance, in one group of the samples, all the other parameters (like nozzle-collector distance, applied voltage, flow rate, etc.) were constant numbers and just the solution concentration differed among the samples of this group. To increase the accuracy of the results, three samples were produced from each differing parameter.

The best electrospinning condition by adjusting parameters of solution concentration, tip-collector distance, applied voltage and flow rate was determined among the

polyurethane nanofiber production trials using electrospinning. For the used polyurethane, the best solution concentration was 10wt% PU/DMF and the applied voltage, nozzle-collector distance and the solution flow rate respectively were 15kv, 15cm and 0.5ml/hr. This process condition gave the fiber morphology with least number of beads.

In case of effects of electrospinning parameters on the fibers diameters, briefly, we conclude that with the concentration and flow rate increase the fiber diameter increases and with the screen distance and electric potential increase the fiber diameter decreases. At very low solution concentrations (4 wt%) a large number of sub-micron droplets were present. At such low concentrations, the viscoelastic force (a result of the low degree of chain entanglements) in a given jet segment was not large enough to counter the higher Coulombic force. Therefore, the charged jet was broken into smaller jets and these smaller jets turned into droplets by rounding as a result of the surface tension. This phenomenon has been used in the industry in applications of paint spraying, ink-jet printing and powder coating and it is termed as electrospraying process.

When high concentrations were used, it was observed that there were nor droplets as the charged jet did not break up into droplets. This could be attributed to the increased chain entanglement and increased viscoelastic force. This suggests that the Coulombic stress elongated the charged jet to the collector. At intermediate concentrations (6wt%, 7wt%, 8wt%), a combination of nanofibers and droplets was observed. As the concentration was further slightly increased (9wt%), the droplets disappeared and a combination of nanofibers and beaded fibers. The beads had an elongated shape.

The longer path length between the nozzle tip and the collector means that there will be a higher probability for the jet segment to thin down as a result of the Coulombic repulsion [Mit-uppatham et al., 2004].

The number of beads created directly depends on the diameters of the produced fibers, with an increase in the fiber diameter, the number of created beads decreases.

## **ELEKTRO LİF ÇEKİM PARAMETRELERİNİN POLİÜRETAN NANOLİF ÇAPI VE LİF MORFOLOJİSİ ÜZERİNE ETKİSİNİN İNCELENMESİ**

### **ÖZET**

Yüksek elektrostatik alanlar pek çok endüstride çok geniş kullanım alanlarına sahiptir [J. Cross, 1987]. Yüksek elektrostatik alan, çapı birkaç nanometreden mikrometrenin alt sınırı arasında değişen ultra ince lifleri üretmek için polimer çözeltilisine veya eriyiğine uygulanabilir. Bu tekniğe elektrostatik lif çekme veya elektro lif çekimi denmektedir. Elektro lif çekimi, çok geniş bir bilim ve teknoloji alanında kullanılan en yeni tekniklerden birisidir. Bu işlem ilk olarak 1897 yılında Rayleigh tarafından gözlemlenmiştir. İşlemin temeli 1969 yılında Taylor tarafından atılmış ve Formahls tarafından düzeneğin çeşitli modelleri patentlenmiştir [Bhardwaj ve ark., 2010]. Son yıllarda, nano ölçekli malzemeler üzerine yapılan araştırmalar son derece basit ve çok yönlü fakat aynı zamanda da ön işlemlerde ve sonraki analiz aşamasında son derece karmaşık olan bu işlem üzerine yoğunlaşmıştır [E. Zdeaveva ve ark., 2011]. Nanolifler çapı  $10^{-9}$  metre olan nano mertebesindeki liflerle ilişkilidir. Genellikle 50 nanometre ve 1 mikron arasında değişen çaplardaki lifler nanolifler olarak kabul edilir, fakat en iyi lifler genellikle en fazla 500 nm çapa sahiptir.

Polüretanlar herbiri en az iki fonksiyonel grup içeren izosiyanatların ve bir alkolün basamaklı (step-growth) polimerizasyonu ile elde edilir [HUCESTE C ve ark., 2001]. Poliüretanlar farklı endüstri alanlarında çok çeşitli uygulamalara sahiptir. Bu uygulamalara örnek olarak otomotiv, inşaat, mobilya, ayakkabı, vb. Sektörlerindeki uygulamalar verilebilir. Günümüzde, poliüretan çözeltilerin özellikle koruyucu tekstiller ve doku mühendisliği uygulamalarında kullanılmak üzere başarılı bir şekilde elektro lif çekimi ile çekilmesine dair çeşitli yayınlar yer almaktadır [E. Zdeaveva ve ark., 2011].

Poliüretan tıpta doku mühendisliği (bağların yeniden konstrüksiyonu), yara örtme, ilaç/gen sevkıyatı, medical malzeme örtüleri, hijyen ve sağlık ürünlerinde kullanılabilmektedir [Bhardwaj ve ark., 2010], [Sheikh, F. A ve ark., 2009], [Han, J. ve ark., 2009].

Elektro lif çekimi düzeneği son derece basittir. Başlıca üç bileşeni yüksek-voltaj güç kaynağı, polimer çözeltisi veya eriyiği için jet olarak kullanılabilecek bir açıklığa da sahip bir hazne ve iletken bir toplama aletidir. Yüksek-voltaj güç kaynağının yayıcı elektrodu polimer çözeltisini veya eriyiğini ya direk olarak elektrodu polimer çözeltisinin veya eriyiğinin içine daldırarak veya elektrodu iletken bir jete bağlayarak

şarj eder. Yüksek-voltaj güç kaynağının diğer veya topraklayıcı elektrodu, çevrimi tamamlamak üzere iletken toplama aletine bağlanır. Elektro lif çekiminde bundan başka düzenekler de mevcuttur [Z. M. Huang ve ark., 2003]. Yayıcı elektrod tarafından polimer çözeltisi veya eriyiğinde oluşturulan aynı polariteye sahip yükler arasındaki Kolomb itme kuvveti, jetin uç kısmında yer alan yarı-küresel şeklindeki damlacığın dengesini bozar ve konik şekilde (Taylor konisi) bir damlacık oluşturur. Elektrostatik alan kuvvetinde kritik bir değerin ötesindeki bir artış ile birlikte, Kolomb kuvveti yüzey gerilmesini geçer. Bunun sonucunda da, polimer çözeltisi veya eriyiğinin elektriksel olarak yüklenmiş akımı (yüklenmiş jet) püskürtülür.

Elde edilen liflerdeki son derece yüksek yüzey alanı/kütle oranına bağlı olarak ve elde edilen nonwoven tülbentlerin mikrometre alt sınırı uzunluk skalasındaki gözeneklerin yüksek yoğunluğuna bağlı olarak, endüstride elektro lif çekimi uygulaması için çok fazla alan bulunmaktadır. Bunların içinde hava ve sıvı filtreleri, yara bantları, doku mühendisliği, yüzey modifikasyonları, ses emici malzemeler, tıbbi ve hijyenik filtreler de yer almaktadır [Kristine Graham, 2002], [Z. M. Huang, ve ark., 2003].

Nanolif teknolojisinin askeri alanda da hafif koruyucu giysi sistemlerinde kullanımı da gelişmektedir. Balistik, kimyasal ve biyolojik korunma için nanolif uygulamaları aktif olarak incelenmektedir. Son yıllarda, nanoteknoloji üzerinde çok geniş araştırmalar yapılmasına rağmen, nanoliflerin termal özellikleri ve soğuk ortamlara karşı koruma potansiyeli nispeten daha az bilinmektedir. Önceki çalışmalar, liflerden yapılmış tabakalardaki ışınlama ısı transferinin 5 ve 10 mikrometre arasındaki lif çaplarında minimum hale geldiğini göstermektedir. Bununla birlikte, son derece küçük çaptaki liflerin veya 1 mikrometreden daha az çaplardaki liflerin ışınlama ısı transferi çok iyi bilinmemektedir. Nanolif içeren ısı izolasyon tabakaları termal koruyucu giysinin ağırlığını ve hacmini azaltabilmekte ve askerlerin savaş alanındaki hareketliliğini artırabilmektedir [Phillip W. Gibson, 2007].

Elektrolif çekimi ile nanolif elde etmede en önemli hedeflerden birisi daha düşük lif çapları ve daha dar lif çapı dağılımına ilaveten daha düzgün lif morfolojisi elde etmektir. Özellikle, nanolifler üzerinde yer alan boncuklu yapı (beads-on-a-string structure) nanolif üretiminde istenmeyen ve minimumda tutulması hedeflenen bir yapıdır. Çözelti konsantrasyonu, düze ve toplayıcı plaka arasındaki mesafe, uygulanan voltaj ve çözelti akış hızı elektro lif çekimi ile elde edilmiş liflerin morfolojik görüntüsünü ve çaplarını direk olarak etkilemektedir. Bu tezin amacı, bu parametrelerin, çalışmada kullanılan termoplastik poliüretandan üretilen nanoliflerin çapı, çap dağılımı ve morfolojisine etkilerini incelemektir.

Çözelti şartlarının morfolojik görünüm ve elektro lif çekimi ile üretilmiş liflerin ortalama çapı üzerine etkileri, nanolif numunelerinin Tarayıcı Elektron Mikroskobu (Scanning Electron Microscope-SEM) görüntüleri alınarak incelenmiştir. Elde edilen görüntüler üzerinde yapılan lif çapı ölçümlerinden ve lifin yapısının incelenmesinden, çözelti konsantrasyonu, düze-toplayıcı plaka mesafesi, uygulanan voltaj ve çözelti akış oranının, önemli etkisi olduğu görülmüştür. Çözelti konsantrasyonunun en fazla etkiye, çözelti akış hızının ise daha az etkiye sahip olduğu gözlenmiştir.

Elektro lif çekimi prose ve çözelti parametrelerinin etkisini incelemek için, parametreler sabit tutularak ve sadece bir parameter değiştirilerek nanolif numuneleri üretilmiştir. Örneğin, bir grupta, düze-toplama plakası arasındaki mesafe, uygulanan voltaj ve akış hızı sabit tutulmuştur ve sadece çözelti konsantrasyonu



değiştirilmiştir. Sonuçların doğruluğunu garantilemek için, her bir tip için 3 adet nanolif demeti tülbenti üretilmiştir.

Poliüretan nanolif elde etmede, uygun çözücü seçimini gerçekleştirmek için tetrahidrofuran (THF) ve dimetilformamid (DMF) çözücüleri ile bunlardan elde edilen çözücü karışımı kullanılarak nanolif üretimi gerçekleştirilmiştir. Yapılan üretim sonucunda en uygun çözücünün DMF olduğu sonucuna varılmıştır. Kullanılan poliüretan için, yapılan denemeler arasında, en düşük lif çapı ve en az boncuklu yapıyı veren işlem parametrelerinin % 10 PU/DMF çözelti konsantrasyonu, 15 KV'luk voltaj, 15 cm'lik düse-toplayıcı plaka mesafesi ve 0.5 ml/saat'lik akış oranı olduğu gözlenmiştir. Elektro lif çekim parametreleri içinde çözelti konsantrasyonu ve akış hızındaki artışın lif çapını artırdığı görülmüştür. Çok düşük konsantrasyonlarda (4 wt%) çok sayıda micron sınırında damlacık mevcuttur. Bu düşük konsantrasyonlarda, bir jet segmentindeki viskoelastik kuvvet (az derecede zincir karmaşasının bir sonucu olarak) daha yüksek Kolomb kuvvetlerine karşı gelecek kadar büyük değildir. Bu nedenle, yüklenmiş jet daha küçük jetlere ayrılmakta ve bu daha küçük jetler de yüzey gerilmesi nedeniyle yuvarlanarak damlacıkları oluşturmaktadır. Bu özellikten endüstride farklı şekilde faydalanılmakta ve elektrospreyleme işlemi de denen bu işlemle boya püskürtme, ink-jet baskı ve tozla kaplama yapılabilir.

Daha yüksek konsantrasyonlar kullanıldığında, yüklenmiş jet damlacıklara ayrılmadığı için damlacık gözlenmemiştir. Bu etki, artan zincir karmaşası ve artmış viskoelastik kuvvete bağlanabilir. Kolomb kuvvetinin yüklenmiş jeti kollektöre doğru uzattığı düşünülmektedir. Ara konsantrasyonlarda (6wt%, 7wt%, 8wt%) ise nanolif ve damlacık kombinasyonundan oluşan bir yapı elde edilmiştir. Konsantrasyon çok az arttırıldığında (9wt%), damlacıklar ortadan yok olmuş ve nanolif ve boncuklu liflerden oluşan bir kombinasyon elde edilmiştir. Elde edilen boncuklu yapıda, boncukların bir kısmının uzatılmış bir şekle sahip olduğu görülmektedir.

Düse-toplayıcı plaka arasındaki mesafe arttıkça lif çapı azalmaktadır. Jet ucu ve toplayıcı plaka arasındaki mesafe ne kadar uzunsa, jet segmentinin Kolomb itme kuvveti sonucu ile incelmeye olasılığı da o kadar yüksektir [Mit-uppatham ve ark., 2004]. Aynı şekilde, uygulanan voltaj arttıkça lif çapı azalmaktadır. Lifler üzerinde görülen boncuklu yapı da işlem parametrelerinden etkilenmektedir. Ayrıca, daha yüksek lif çaplarında boncuk sayısının arttığı görülmüştür.



## 1. INTRODUCTION

The fast spreading of the research in the field of nanotechnology in the past decades has brought along the need of electrospinning technique, which is an older method.

High electrostatic fields can be applied to either polymer solutions or melts to produce non-woven webs of ultrafine fibers, the diameters of which are in the range of few nanometers to sub-micrometers [A. Formhals, 1934], [A. Formhals, 1944]. Such a technique is called electrostatic spinning or electrospinning.

Electrospinning is one of the most recent techniques, which has been used in a vast field of science and technologies. This method uses a high electrical charge to draw very fine (typically on the micro or nano scale) fibers from a liquid. This liquid is always the polymer solution or its melt. The process was first observed by Rayleigh in 1897. The basis was laid by Taylor in 1969, and various models of the set up were patented by Formahls 1934-1944 [Bhardwaj et al, 2010]. In the past years the investigation of nanoscaled materials has intensified the interest in this very simple and versatile process, but yet very complex in its pre-process and after analysis [E. Zdeaveva et al, 2011]. Nanofibers refers to the fibers with the diameters in the nano scale which is  $10^{-9}$  meter [S. R. Singh, 1995]. Usually fibers with diameters from 50 Nanometer to 1 micron are acceptable as nanofibers but the best fibers usually have 100-500 Nm diameters.

Polyurathanes are synthetic polymers made by a step-growth polymerization of isocyanates and an alcohol both with at least two functional groups. Polyurethanes have a vast range of applications in different industry fields, eg. automotive, construction, furniture, footwaer etc. Nowadays there are number of studies that reported on the successful electrospinning of polyurethane solutions, especially for the purpose of protective textiles and tissue engineering applications [E. Zdeaveva et al, 2011].

TPU (Termoplastic Polyurethane) is typically used for parts requiring a high level of performance. Applications typically require a flexible material with a high degree of

flex resistance, wearability and durability. Many of the characteristics of TPU make it ideal for medical use. Medical applications include site dressing, transdermal patches, thin film wound dressings, cast and dressing covers, surgical gowns and drapes, puncture-resistant gloves, incontinence pads, compression dressings, orthopedic gel insoles, medical anti-shock trousers, gel-filled positioning pads, inflatable support bladders, pressure infuser cuffs, extraction bags, hospital mattresses, covers and orthodontic brace aligners.

There is a vast field of nanofiber applications on recent nanotechnology science and it is dramatically growing now days. Due to the exceptionally high surface area to massratio of the fibers obtained and the high density of pores on the sub-micrometer length scale of the obtained non-wovenwebs, proposed applications for electrospun products are in areas where these properties are fully utilized. Air and liquid filters, wound dressings, tissue engineering, surface modifications, sound absorptive materials and industrial, medical and hygienic filtrations are some examples of nanofiber applications[Kristine Graham, 2002], [Z. M. Huang, et al ,2003].Nanofiber technology is developping gradually for army lightweight protective clothing systems. Nanofiber applications for ballistic, chemical and biological protection are being actively investigated, although in recent years vast investigations on nano technology were done, the thermal properties of nanofibers and their potential protection against cold environments are relatively unknown. Previous studies have shown that radiative heat transfer in fibrous battings is minimized at fiber diameters between 5 and 10 micrometers. However, the radiative heat transfer mechanism of extremely small diameter fibers of less than one micrometer diameter is not well known. Previous studies were limited to glass fibers, which have a unique set of thermal radiation properties governed by the thermal emissivity properties of glass.Thermal insulation battings incorporating nanofibers could decrease the weight and bulk of current thermal protective clothing, and increase mobility for soldiers in the battlefield. [Phillip W. Gibson, 2007].

The term morphology is generally attributed to the German poet, novelist, playwright, and philosopher Johann Wolfgang von Goethe (1749–1832), who coined it early in the nineteenth century in a biological context. Its etymology is Greek: morph- means ‘shape, form’, and morphology is the study of form or forms. In biology morphology refers to the study of the form and structure of organisms, and in

geology it refers to the study of the configuration and evolution of land forms. In linguistics morphology refers to the mental system involved in word formation or to the branch of linguistics that deals with words, their internal structure, and how they are formed[Mark Aronoff and Kirsten Fudeman, 2010].

In textile, morphology refers to the study of the microscopic structure of fibers and their distribution and alignment. In nanofiber investigations due to their nanoscale structure, morphology has a great importance, because observing the fibers distribution, alignment and measuring the fibers diameters and the number of created beads, play a very important role to determine the produced fibers quality (because our aim always is to obtain minimum fiber diameter with no or less beads) and without armed eyes and morphology studyings, obtaining such a result is impossible.

The most important process parameters in electrospinning process are: solution concentration, nozzle-collector distance, applied voltage and solution flow rate. Solution concentration has been proved in most literatures to be the most important one amongthe other parameters. Briefly, with the concentration and flow rate increase the fiber diameter increases and with the screen distance and electric potential increase the fiber diameter decreases[Audrey Frenot et al, 2003]. These results are of interest because processing parameters influencing droplet size and size distribution in the electrospray process may similarly influence the morphology of polymer fibers formed using the electrospinning process [Deitzel et al, 2001].

### **1.1. Purpose of Thesis**

The purpose of this study was to determine the best solution concentration for thermoplastic polyurethane and its solvents, also determination of the best nozzle-collector distance, feeding rate and the best voltage amount of the electrospinning machine, also to investigate the coating ability of TPU nanofibers.



## **2. LITERATURE REVIEW**

### **2.1. Electrospinning and the Process Description:**

Production of synthetic fibers using electrostatic forces has been known for more than hundred years. The process of spinning fibers under an electric field using electrostatic force is known as electrospinning [Thandavamoorthy Subbiah et al, 2005]. Electrospinning is a simple and low-cost method for making ultrafine fibers with diameters ranging from several micrometers to several hundreds of nanometers using a high-voltage D.C. electric source [Heikkila P and Harlin A, 2008]. This method is a process used to fabricate continuous nanoscale fibers with diameters in the sub-micrometer to nanometer range ( $10^{-6}$  m –  $10^{-9}$  m) using a high-voltage power supply [Cungang-ro et al, 2011]. Electrospun fibers have small cross section and high surface area and because of these properties of nanofibers, there is a wide range of applications using these fibers. Electrospinning is a process by which a polymer solution or melt can be spun into smaller diameter fibers using a high potential electric field. Under this electric field, the fluid elongates from a nozzle tip and its being ejected by increasing the field intensity, This generic description is appropriate as it covers a wide range of fibers with submicron diameters that are normally produced by electrospinning. The average diameter of electrospun fibers ranges from 100 nm–500 nm [Thandavamoorthy Subbiah et al, 2005]. The process was first observed by Rayleigh in 1897, the basis were laid by Taylor in 1969., and various models of the set up were patented by Formahls 1934-1944 [Bhardwaj N. and Kundu S. C., 2010]. In the past years the investigation of nanoscaled materials has intensified the interest in this very simple and versatile process, but yet it is very complex in its pre-process and after analysis.

The construction of the apparatus which is used for electrospinning is relatively simple, which consists of a high voltage electric supplier with positive or negative polarity, a syringe pump with capillaries or tubes to carry the solution from the

syringe or pipette to the spinnerette, and a conducting collector like aluminum or any kind of other conductive metals. The collector can be made of any shape according to the requirements, like a flat plate, rotating drum, etc [Thandavamoorthy Subbiah et al, 2005]. A schematic of the electrospinning setup is shown in Figure 1.

Currently, there are two standard electrospinning setups, vertical and horizontal. With the expansion of this technology, several research groups have developed more sophisticated systems that can fabricate more complex nanofibrous structures in a more controlled and efficient manner [Kidoaki S et al, 2005], [Stankus JJ et al, 2004]. Electrospinning is conducted at room temperature with atmosphere conditions. Basically, an electrospinning system consists of three major components: a high voltage power supply, a spinneret (e.g., a pipette tip) and a grounded collecting plate (usually a metal screen, plate, or rotating mandrel) and utilizes a high voltage source to inject charge of a certain polarity into a polymer solution or melt, which is then accelerated towards a collector of opposite polarity [Liang D et al, 2007], [Sill TJ et al, 2006].

Most of the polymers are solvable in some solvents and are dissolved before electrospinning, and when it completely dissolves, forms polymer solution. The polymer fluid is then introduced into the capillary tube for electrospinning. However, some polymers may emit unpleasant or even harmful smells, so the processes should be conducted within chambers having a ventilation system [Huang ZM et al, 2003].

In the electrospinning process, a polymer solution held by its surface tension at the end of a capillary tube is subjected to an electric field and an electric charge is induced on the liquid surface due to this electric field. When the electric field applied reaches a critical value, the repulsive electrical forces overcome the surface tension forces.

Eventually, a charged jet of the solution is ejected from the tip of the Taylor cone and an unstable and a rapid whipping of the jet occurs in the space between the capillary tip and collector which leads to evaporation of the solvent, leaving a polymer behind. The jet is only stable at the tip of the spinneret and after that instability starts. Thus, the electrospinning process offers a simplified technique for fiber formation [Taylor GI et al, 2011], [Yarin AL et al, 2001], [Adomaviciute E et al, 2007].



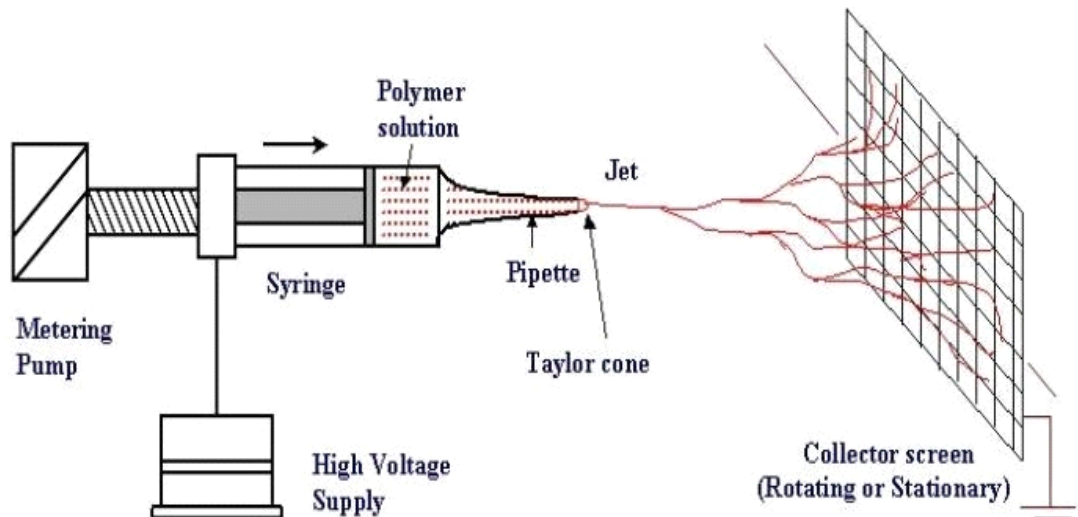


**Figure 2.1 : The Electrospinning Setup**

The setup of the electrospinning process is very simple. The three major components are a high-voltage power supply, a container for a polymer solution or melt with a small opening to be used as a nozzle and a conductive collection device. An emitting electrode of the high-voltage power supply charges the polymer solution or melt by either directly submerging the electrode in the polymer solution or melt or by connecting the electrode to a conductive nozzle. The other or grounding electrode of the high-voltage power supply is connected to the conductive collection device to complete the circuit. Other setups are also possible [Z. M. Huang et al, 2003]. The Coulombic repulsion force between charges of the same polarity produced in the polymer solution or melt by the emitting electrode destabilizes the hemi-spherical droplet of the polymer solution or melt located at the tip of the nozzle to finally form a droplet with a conical shape (i.e. the Taylor cone). With further increase in the electrostatic field strength beyond a critical value, the Coulombic repulsion force finally exceeds that of the surface tension which results in the ejection of an electrically charged stream of the polymer solution or melt (the charged jet).

There are six major forces acting on an infinitesimal segment of the charged jet. They are 1) body or gravitational forces, 2) electrostatic forces which carry the charged jet from the nozzle to the target, 3) Coulombic repulsion forces which try to push apart adjacent charged species present within the jet segment and are responsible for the stretching of the charged jet during its flight to the target, 4) viscoelastic forces which try to prevent the charged jet from being stretched, 5)

surface tension which also acts against the stretching of the surface of the charged jet and 6) drag forces from the friction between the charged jet and the surrounding air [L.Wannatong et al, 2004]. Due to the combination of these forces, the electrically charged jet travels in a straight trajectory for only a short distance before undergoing a bending instability, which results in the formation of a looping trajectory [D. H. Reneker et al, 1996], [D. H. Reneker et al, 2000]. During its flight to the collector, the charged jet thins down and, at the same time, dries out or solidifies to leave ultrafine fibers on the collective screen.

Briefly, In the electrospinning process, a polymer solution is charged using a high-voltage power supply and the volume feed rate controlled using a capillary pump. Once the electric field reaches a critical value at which the repulsive electric force overcomes the surface tension of polymer solution, the polymer solution is ejected from the tip to a collector. While traveling to the collector, the solution jet solidifies due to the fast evaporation of the solvent and is deposited on a collector [Cungang-ro et al, 2011].

Some problems would be found when electrospinning blends of two chemically different polymers, in which the polymer blend solutions are not homogenous owing to the different solvent system of the two polymers. One way to overcome these complicated issues is to electrospin two polymer solutions simultaneously using a coaxial electrospinning technique, as shown in Figure 2. E-spun fibers made using the coaxial electrospinning technique have a bicomponent system that has properties from each of the polymeric components e.g. one of the polymers could contribute to the mechanical strength while the other could enhance the wettability of the resulting non-woven web.

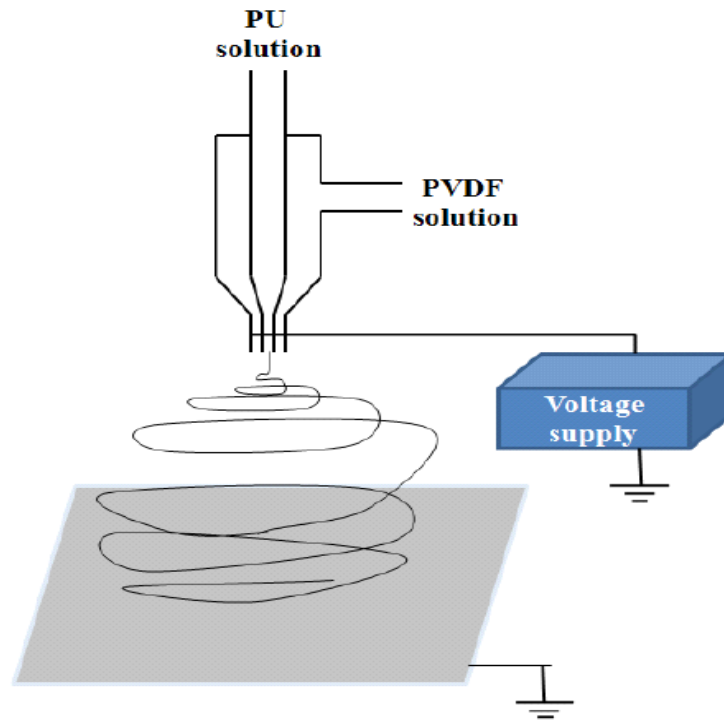


**Figure 2.2 :** Schematic Diagram of a Coaxial Electrospinning Apparatus.

## 2.2. Electrospinning Applications:

There is a vast field of nanofiber applications on recent nanotechnology science and it is dramatically growing nowadays. Due to the exceptionally high surface area to mass ratio of the fibers obtained and the high density of pores on the sub-micrometer length scale of the obtained non-woven webs, proposed applications for electrospun products are in areas where these properties are fully utilized. Air and liquid filters, wound dressings, tissue engineering, surface modifications, sound absorptive materials and industrial, medical and hygienic filtrations are some examples of nanofiber applications [Kristine Graham, 2002], [Z. M. Huang, et al, 2003]. Nanofiber technology is developing gradually for Army lightweight protective clothing systems. Nanofiber applications for ballistic, chemical and biological protection are being actively investigated, although in recent years vast investigations on nano technology were done, the thermal properties of nanofibers and their potential protection against cold environments are relatively unknown. Previous studies have shown that radiative heat transfer in fibrous battings is minimized at fiber diameters between 5 and 10 micrometers. However, the radiative heat transfer mechanism of extremely small diameter fibers of less than 1 micrometer diameter is not well known. Previous studies were limited to glass fibers, which have a unique

set of thermal radiation properties governed by the thermal emissivity properties of glass. Thermal insulation battings incorporating nanofibers could decrease the weight and bulk of current thermal protective clothing, and increase mobility for soldiers in the battlefield, [Phillip W. Gibson, 2007].

Owing to the useful properties of electrospun fibers, many synthetic and natural polymers, including single and blended polymers, have been electrospun into fibers that can be employed in a variety of applications, such as filtration and thermal insulation, and in the manufacture of protective clothing, sensors, conducting devices, wound dressings and scaffolds for tissue [Heikkila P and Harlin A, 2008], [Varesano A et al, 2009]. (Figure 3)

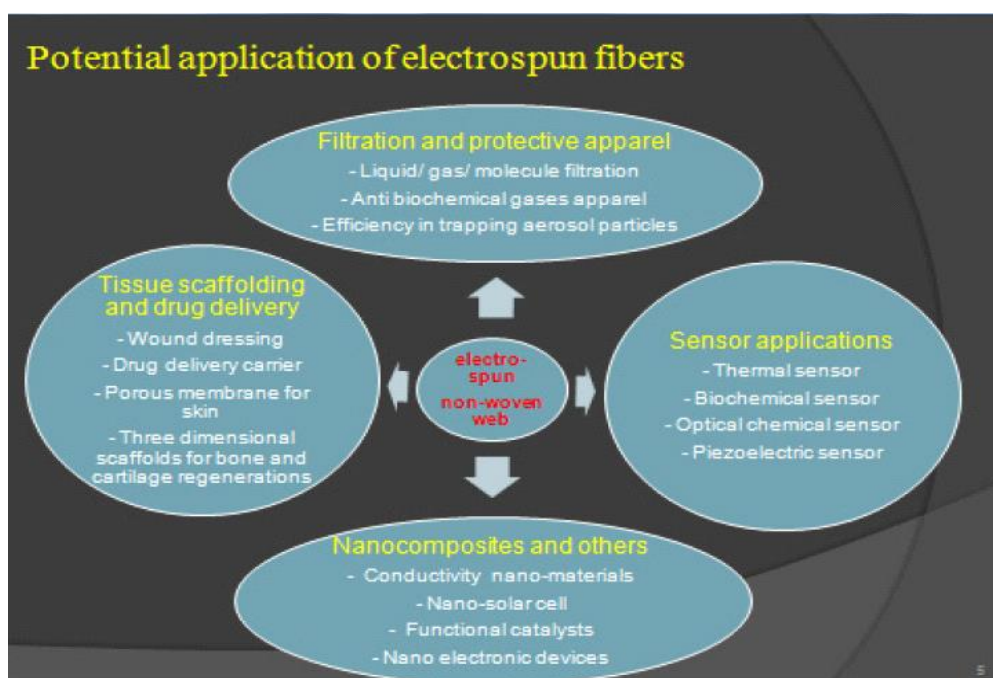


**Figure 2.3 : Electrospun Fibers Applications**

Chitosan(CS),is one of the most abundant natural polysaccharides that have non-toxic, biodegradable properties. One useful property of Chitosan (CS) is its antibacterial activity, which means that it can be used in wound dressing, drug delivery systems, antimicrobial applications, membrane filtration and various tissue-engineering applications [Cungang-ro et al, 2011].

Due to the requirement of developing more renewable and clean energy sources, phase change materials (PCMs) have gained much attention for several decades [Mondal S, 2008]. PCMs can absorb energy during the heating process and release energy to the environment during a reverse cooling process as a phase change takes

place [Cungang-ro et al, 2011]. When PCMs are directly used as a heat storage material, there are some inherent drawbacks such as density changes, phase segregation, low thermal conductivity and leaking. Encapsulation of the PCMs is as an effective alternative. Due to their small diameter, which is from less than 1 $\mu$ m to more than 300 $\mu$ m, the ratio of surface area to volume of the microencapsulated PCM is high and thermal conductivity also increases. In the fabrication of thermo-regulating composite fibers, the PCMs' polymer blended solution can directly electrospun. Non-woven mats that contain PCMs and supporting materials (polymers) have some attractive advantages, such as not requiring additional encapsulation, desirable dimensions, high latent heat, mechanical strength and specific surface area. However, a shortcoming of the fibers fabricated using this method is that the PCMs in the fibers could easily be lost in use. Based on the electrospinning principle, the coaxial electrospinning uses a spinneret composed of two coaxial capillaries to fabricate continuous double layer nanofibers. polyethylene glycol (PEG)/polyvinylidene fluoride (PVDF) core/sheath non-woven mats can prepared using coaxial electrospinning in which PEG formed the core and PVDF made the sheath of nanofibers [Cungang-ro et al, 2011].

While the complex whipping motion of a typical electrospinning jet results in a nonwoven mat of fibers, there have been many developments aimed at controlling the deposition of an electrospinning jet to form more ordered patterns of nanofibers. Such controlled deposition is desirable as it would provide a low-cost fabrication technique for nanoscale devices such as nanomechanical devices, electronic devices, and light-emitting systems.

Nanofibers may also be used as masks or templates to create nanoscale structures in other materials. Other modifications to a standard electrospinning system allow for a typical nanofiber morphologies such as hollow or coaxial nanofibers, side-by-side nanofiber deposition, etc [Leon M. Bellan and Harold G. Craighead, 2010].

### **2.3. Electrospinning Process Parameters**

In the electrospinning process of a polymer solution, a number of parameters can influence the morphology of the obtained fibers. These governing parameters can be categorized into three main types: 1) solution (e.g. concentration, viscosity, surface tension and conductivity of the polymer solution), 2) process (e.g. applied

electrostatic potential, collection distance and feed rate) and 3) ambient parameters (e.g. temperature, relative humidity and velocity of the surrounding air in the spinning chamber) [Z. M. Huang et al, 2003], [J. Doshi et al, 1995]. Baumgarten was one of the early researchers who recognized the effects of some of these parameters on the morphological appearance of as-spun acrylic fibers. He found that an increase in the solution viscosity (as the result of an increase in the solution concentration) was responsible for an increase in the average fiber diameter, while an increase in the flow rate of the acrylic solution did not appreciably affect the fiber diameters [P. K. Baumgarten, 1971].

The production of nanofibers by the electrospinning process is influenced both by the electrostatic forces and the viscoelastic behavior of the polymer. Process parameters, like solution feeding rate, applied voltage, nozzle-collector distance, and spinning environment, and material properties, like solution, viscosity, surface tension, conductivity, and solvent vapor pressure, influence the structure and properties of electrospun nanofibers [Thandavamoorthy et al, 2005]. These results are of interest because processing parameters influencing droplet size and size distribution in the electrospray process may similarly influence the morphology of polymer fibers formed using the electrospinning process [Deitzel et al, 2001].

The following parameters and processing variables affect the electrospinning process: (i) System parameters such as molecular weight, molecular-weight distribution and architecture (branched, linear etc.) of the polymer and solution properties (viscosity, conductivity and surface tension), and (ii) Process parameters such as electric potential, flow rate and concentration, distance between the capillary and collection screen, ambient parameters (temperature, humidity and air velocity in the chamber) and finally motion of target screen [WilkesGL, 2001].

For instance, the polymer solution must have a high enough concentration to cause polymer entanglements and not so high that causes the viscosity to prevent polymer motion induced by the electric field. The solution must also have a surface tension low enough, a charge density high enough, and a viscosity high enough to prevent the jet from collapsing into droplets before the solvent has evaporated. Morphological changes can occur upon decreasing the distance between the syringe needle and the substrate. Increasing the distance or decreasing the electrical field decreases the bead density, regardless of the concentration of the polymer in the

solution. Applied fields can, moreover, influence the morphology in periodic ways, creating a variety of new shapes on the surface [Audrey Frenot and IoannisS. Chronakis, 2003].

Deitzel et al. have evaluated systematically the effects of two important processing parameters, spinning voltage and solution concentration, on the morphology of the fibers formed [Deitzel JM et al, 2001]. They found that spinning voltage is strongly correlated with the formation of bead defects in the fibers, and their measurements can be used to signal the onset of the processing voltage at which the bead defect density increases substantially. Solution concentration has also been found to most strongly affect fiber size, with fiber diameter increasing with increasing solution concentration according to a power law relationship. In addition, electrospinning from solutions of high concentration has been found to produce a bimodal distribution of fiber sizes, reminiscent of distributions observed in the similar droplet generation process of electrospray. Moreover they found evidence that electrostatic effects influence the macroscale morphology of electrospun fabrics and may result in the formation of heterogeneous or three-dimensional structures [Audrey Frenot and IoannisS. Chronakis, 2003].

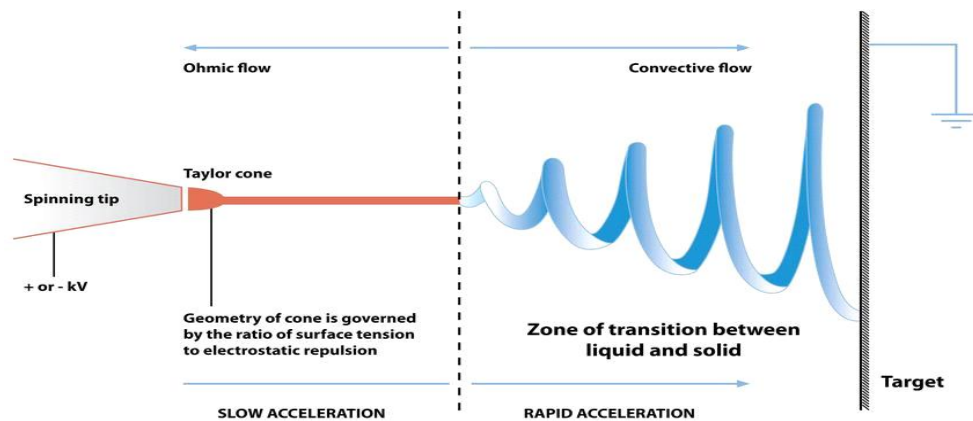


**Figure 2.4 :** Electrospinning Flow Between Different Zones

We conclude that, (i) fibers of different sizes, i.e. consisting of different numbers of parent chains, exhibit almost identical hyperbolic density profiles at the surfaces, (ii) the end beads are predominant and the middle beads are depleted at the free surfaces, (iii) there is an anisotropy in the orientation of bonds and chains at the surface, (iv) the centre of mass distribution of the chains exhibits oscillatory behaviour across the



fibers and (v) the mobility of the chain in nanofiber increases as the diameter of the nanofiber decreases [Audrey Frenot and Ioannis S. Chronakis, 2003].

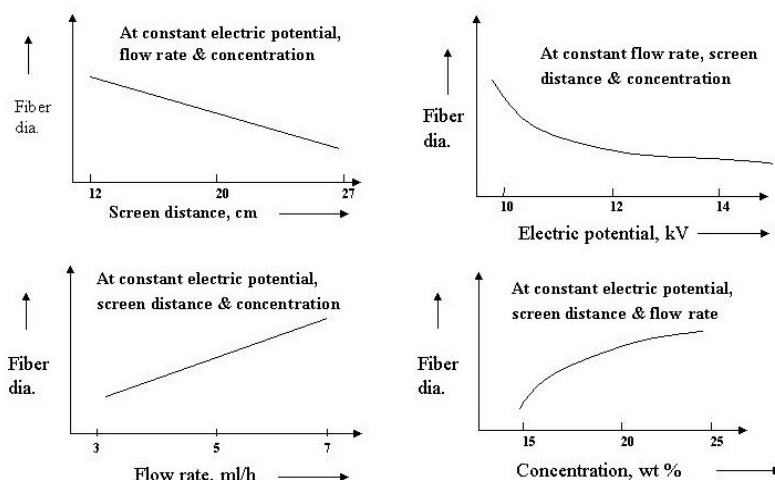


**Figure 2.5 :** Effects of Process Parameters on Fiber Diameter

Doshi and Reneker classified the parameters that control the process in terms of solution properties, controlled variables, and ambient parameters.

Solution properties include the viscosity, conductivity, surface tension, polymer molecular weight, dipole moment, and dielectric constant. The effects of the solution properties can be difficult to isolate since varying one parameter can generally affect other solution properties (e.g., changing the conductivity can also change the viscosity). Controlled variables include the flow rate, electric field strength, distance between tip and collector, needle tip design, and collector composition and geometry. Ambient parameters include temperature, humidity, and air velocity. In this section, studies that investigate the effect of each parameter on electrospun fiber morphologies and sizes are highlighted [Doshi, J. et al, 1995], [Deitzel et al, 2001].

Briefly, The most important process parameters in electrospinning process are: solution concentration, nozzle-Collector distance, applied voltage and solution flow rate. solution concentration has been proved in most literatures to be the most important parameter between the other parameters, literature review proved that with the concentration and flow rate increase the fiber diameter increases and with the screen distance and electric potential increase the fiber diameter decreases [Audrey Frenot et al, 2003].



## 2.4. PU (Polyurethane) Nanofibers Obtained by Electrospinning:

Polyurethanes are synthetic polymers made by a step-growth polymerization of isocyanates and an alcohol both with at least two functional groups (*Soljacic I. 1993*) (Figure 5). Polyurethanes have a vast range of applications in different industry fields, e.g. automotive, construction, furniture, footwear etc (*Introduction to polyurethanes*). Nowadays there are number of studies that report on the successful electrospinning of polyurethane solutions, especially for the purpose of protective textiles and tissue engineering applications [E. Zdeaveva et al, 2011].

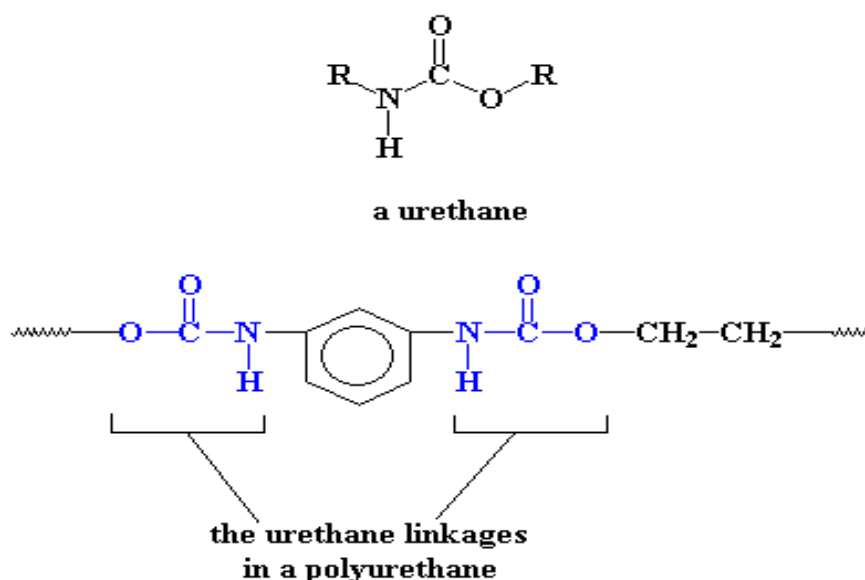


**Figure 2.6 :** Step-Growth Polymerization of Polyurethane

PU can be used in medicine tissue engineering (ligament reconstruction), wound dressing, drug/gene delivery, to cover medical devices, materials for sanitation and health care [Bhardwaj et al, 2010], [Sheikh, F. A et al, 2009], [Han, J. et al, 2009]. Among PUs, there is one group of very promising smart materials called shapememory PU. They can change their shape, hydro absorbency, water vapor permeability, stable of water, selfcleaning ability, optical and other properties when external change. Also PU can be used for production in high-efficiency filters, protective textiles, sensors, food packaging, and biosensors [Sheikh, F.A. et al, 2009], [Han, J. et al, 2009],[Chen, M. et al, 2007]. Thermoplastic polyurethane (TPU) is used in medicine for good compatibility with blood, also it can be used as

heart valves, ventricular frame. TPU presents a class of polymers that possess a range of very desirable properties: they are elastomeric, resistant to microorganisms and abrasion and have excellent hydrolytic stability [Pedicini, A. et al, 2003]. TPU can be dissolved in tetraethylammoniumbromide, N,N-dimethylformamide, dimethylacetamide, ethanol, tetrahydrofuran, and mixtures [Rockwood, D. N. et al, 2008], [Cengiz, F., et al, 2009]. TPU viscous state is achieved by heating it to about 120 °C temperature [Kang Y. K. et al, 2007].

Laminated fabric with polyurethane coating with nanopores is a multilayered composite material. Textile composite materials are composed of two or more different materials with at least one textile layer (woven fabric, knitted fabric or nonwoven material). All components composing the final product affect the properties of multilayered composites. The portion of individual components can be different which enables obtaining a composite with target properties for the predetermined purpose. Nowadays the material with woven fabric on the front side and polyurethane with nanopores on the back side is mostly used for military or police outerwear as well as for civil uses. For military purposes camouflage fabric in different shades and designs or less frequently single colored is used, while single colored fabrics in blue shades are used for police purposes. This kind of composites have multiple advantages over the classic fabric since they are more durable and stronger, their body protection against meteorological effects (rain, wind, UV radiation), they did not lose their comfort (they are airy and have good sweat permeability), they are more resistant to abrasion and load, and they have less anisotropic properties in contrast to the classic fabrics [Stana Kovačević et al, 2001].

Properties of composites with the woven fabric as the basis depend to a great extent on weave type, warp and weft density, yarn count and the angle of the straight line under which the load acts in relation to the warp and weft direction. The highest breaking strength is expected in the warp direction and then in the weft direction. According to the previous investigations the stress of the composite material with the woven fabric outside the warp and weft direction considerably reduces fabric breaking force. Through the action of the external force on the composite material the internal cohesion forces resist more strongly to the warp and weft direction in relation to other directions. The relaxation of the internal forces in the state of stress begins earlier if the force acts under a certain angle in relation to the warp and weft

direction. This phenomenon defines fabric anisotropy which reflects on the composite material with one or more fabric layers. Load is expressed as the ratio of the internal forces acting on the area unit of the sample [P. Durst, 1985], [D. Jakšić, 1994].

J. E. Sanders with co-authors have analyzed the polyurethane (PU) (Estane 58315, BF Goodrich, Cleveland, OH), polyester (PES), polyethylene (PET) and poly(L-lactic acid) (PLA) electrospun microfibers diameter. During this study it was estimated that the percentage of fibers with diameter 1  $\mu\text{m}$  – 5  $\mu\text{m}$  was greater for PET and PU (75.0 % and 71.4 % respectively) than for PE and PLA (45.5 % and 56.3 % respectively) [Sanders, J. E. et al., 2002].

D. Cha with co-authors researched the dependence of shape-memory PU block copolymers fibers diameter upon solution concentration and viscosity. It was stated that the PU fibres electrospun from lower viscosity (ca. 130 cPs – 180 cPs) had diameter about 800 nm and a beaded-on-fiber structure. In contrast, the samples spun at a higher PU solution viscosity (ca. 530 cPs – 570 cPs) showed a smooth fiber surface with an average diameter about 1300 nm. The electrospun PU nonwovens with a hard-segment concentration of 50 wt.% had higher stress than those with a hard segment concentration of 40 wt.% [Cha, D. I. et al., 2005].

M. M. Demir with co-authors have studied that PU (based on poly(tetramethylene oxide) glycol, a cycloaliphatic diisocyanate and an unsymmetrical diamine fiber diameter increase as the third power of solution concentration. Low concentration solutions drive towards the formation of fibers with beads, whereas increased concentration favors the formation of curly PU fibers [M. M. Demir et al., 2002].

Study reported on polyurethane/urea solution electrospun into fibers with diameters in the range of 7 nm to 1.5  $\mu\text{m}$ . Fibers spun at lower solution concentration were noted to have beads and at high concentrations resulted in curliness. Higher than room temperatures conditions improved the fibers imperfections (Demir M. M. et al. 2002.). Another study reported on polyurethane/collagen electrospun fibers through coaxial spinneret as well as both pure polymers separately (Chen R. et al. 2010.). It was observed that a range of solution concentration between 3-6 wt% of the core PU structure provided smooth fibers, higher concentration increased the fibers diameters. Improving solution conductivity obtained smaller diameters [E. Zdeaveva et al., 2011].

## 2.5. Characterization of Nanofibers



**Figure 2.7 :** SEM (Scanning Electron Microscope)

When the diameters of polymer fiber materials are shrunk from micrometers (e.g. 10–100  $\mu\text{m}$ ) to submicrons or nanometers (e.g.  $10 \times 10^{-3}$  –  $100 \times 10^{-3} \mu\text{m}$ ), there appear several amazing characteristics such as very large surface area to volume ratio (this ratio for a nanofiber can be as large as  $10^3$  times of that of a microfiber), flexibility in surface functionalities, and superior mechanical performance (e.g. stiffness and tensile strength) compared with any other known form of the material. These outstanding properties make the polymer nanofibers to be optimal candidates for many important applications.

A number of processing techniques such as drawing [Ondarcuhu T et al, 1998], template synthesis [Feng L et al, 2002], [Martin CR, 1996], phase separation [Ma PX, Zhang R. , 1999], self-assembly [Liu GJ, Ding JF et al, 1999], [Whitesides GM, Grzybowski B, 2002], electrospinning [Deitzel JM et al, 2001], [Fong H, Reneker DH, 2001], etc. have been used to prepare polymer nanofibers in recent years.

To observe and investigate these characterizations we need to utilize the scanning electron microscope and without SEM it is impossible to calculate and observe the exact fiber diameters, distribution and alignment of fibers, number of beads created and generally the morphology of the fibers.

A scanning electron microscope (SEM) is a type of electron microscope that produces images of a sample by scanning over it with a focused beam of electrons. The electron microscope (EM) is a scientific instrument that utilizes a beam of

electrons, rather than light, to image a specimen. Electron microscopes (EM) have a large depth of field and provide a high level of magnification. The quality and clarity of details of the image are dependent on resolution, and the resolution achieved by electron microscopes ranges between 2- 20 angstroms. Scanning electron microscopy (SEM) magnifies specimens pertaining to biology, medicine, matter sciences and earth sciences, 100 000 times, and enables evaluation of differences in the surface by means of imaging surface structures. SEM reconstructs a visionary three-dimensional image.

When a beam of primary electrons strikes a bulk solid, the electrons are either reflected or absorbed, producing various signals. The incident electrons spread into a pear-shaped volume in the solid. Backscattered electrons (BSE), x-rays and other responses are produced as well as secondary electrons (SE). The most frequent modes in the SEM involve the capture of secondary and backscattered electrons. Modern SEMs may include energy dispersive x-ray (EDX) and wavelength dispersive (WD) analyser which gives a more detailed information about the sample.

SEM can reveal topographical details of a surface with clarity and detail which cannot be obtained by any other means. It can resolve the topographical details of less than 50 Å with a depth of focus 500 times that of an optical microscope at equivalent magnification. The high linearity of raster scanning of beam, at a magnification over few thousands, resulting in a constant magnification over the entire image. This allows us very precise size measurements after calibration. An analytical scanning electron microscopy (SEM/EDS) provides: (1) Secondary electron images of surface features to ~ 50 Å in resolution, (2) Backscattered electron images of phase differentiation, precipitates, reaction regions etc. based on average atomic number contrast, (3) Topographic images of pits, protrusions, reacted regions etc., (4) Surface potential distribution, (5) Surface conductivity, (6) Crystallography, (7) Scanning maps of elemental distribution in near surface region normally for elements above F, i.e., not for C, N, O, and (8) Quantitative analysis, with standards, for comparison with assays, XPS etc [S. R. Singh, 1995].

## **2.6. Predictions:**

According to chart 1 from laterator rewive, approximately 20cm nozzle-collector distance is expected due to the possibility of creation of beads after this distance, because with augmentation of distance the fiber diameter decreases and with fiber diameter reduction the possibility of bead production increases.

We predict that the electric potential would be approximately around 12kv due to the chart below with augmentation of electric voltage the fiber diameter will decrease and it causes the creation of beads (our goal is to produce finnest finers with no or less beads).By the same logic, we can conclude that the appropriate flow rate would be 4ml/Hr and the appropriate concentration would be 15wt%.

For fabric coating with polyurethane nanofibers we expect that the fabrics water permeability would dramatically decrease but the fabrics air permeability would almost be a constant number because of the low fiber diameter of nanofibers the created pores between the fibers will be very small and due to the pores sizes, it would be difficult for water molecules to penetrate into the fabric structure but because of the smaller size of the air molecules and water cohesion and adhesionproperties (comparing with the water molecules), penetrating into the fabric structure would not be difficult.

### 3. EXPERIMENTAL WORK

Although it has been shown in a recent review by Huang and co-workers [Z. M. Huang, 2003], that various aspects of electrospun fibers have been intensely explored and reported in the open literature in the past, a number of fundamental aspects of the process for different polymer-solvent systems are still worthy of further investigation in order to gain a thorough understanding of the process.

#### 3.1. Materials and Chemicals

The electyrosinning device used in this thesis consists of syringe, a metering pump, a High Electric Voltage Supply and a collector. The glass syringe has a capacity of 2 ml. The metering pump was from New Era Pump System Inc and its model was NE-300 (Volts/Hz=12VDC and Amperage of 0.75). A Gamma High Voltage Research ES50P power supply was used to charge the spinning PU solutionsby connecting the emitting electrode of positive polarity to thenozzle and the grounding electrode to the collective screen.A piece of thick aluminium (Al) sheet was used as a collective screen.



**Figure 3.1 : A Set of an Electrospinning Machine**

The utilized polymer was thermoplastic polyurethane 1660 LARICOL from Coim company. Technical specifications of the utilized polymer is given in chart 2.

**Table 3.1 :** The technical specifications of the utilized polymer

	1660
Minimum reactivation temperature	50/55
Open time	Medium
Crystallization rate	Medium
Thermal resistance	Very good
Cold resistance	Medium
Resistance to fats oils and plasticizers	Good

**Table 3.2 :** LARICOL Solubility/Viscosity in Various Solvents Related to MEK

	LCL 1660
MEK	1
Acetone	0.9
THF	1.7 – 1.9
Dioxane	7 – 9
Cyclohexanone	6.5 – 8.5
Toluene	R
Methylene chloride	R
1, 1, 1, chloroEthane	R
Ethyl acetate	R
Trichloroethylene	R
MEK = Toluene	1.3 – 1.5 (9:1)
MEK = Ethyl Acetate	1.4 – 1.6 (8:2)
MEK = Methylene Chloride	VG (9:1)



**Table 3.3 : Physical and Chemical Properties of Utilized PU**

Appirance and Colour	White granule
Odour	Absent
pH:	n.a.
Melting point	n.a.
Boiling point	n.a.
Flash point	n.a.
Non volatile content	100
Bulk density	700 kg/m <sup>3</sup>
Specific gravity	1.2 g/cm <sup>3</sup>
Solubility in water	Not soluble

DMF (Dimethylformamide) and THF (Tetrahydrofuran) were used as the solvents in the electrospinning process. TPU (thermoplastic polyurethane) was dissolved by using these solvents.

### 3.2. Application Data

In all the experiments when the other parameters are not given means that we were used our best amounts of variables, which are: 10wt% concentration, 15cm nozzle-collector distance, 15 kilovolt applied voltage and 0.5 ml/hr flow rate. For example, for the 12wt% sample, the applied voltage is 15kv, the nozzle-collector distance is 15cm and the flow rate is 0.5 ml/Hr.

The laboratory situations were standard laboratory situations, which are 25 °C temperature and 1 Atm air pressure. Each polymer solution dissolved approximately in one hour and each sample exposed to the electrospinning machine for half an hour.

### 3.3. Utilized Scanning Electron Microscope's Characterizations:

All the micrographs were taken with the ZEISS, EVO MA10 model, Scanning Electron Microscope in Ali Demir Laboratory of Mechanical Engineering faculty of Istanbul Technical University, some of the key features of this microscope are:

- Variable pressure operation

- Large stage movements
- Fast pump down
- 4 quadrant and 5 segment backscatter imaging
- Future Assured upgrades to water vapor enhanced imaging
- High brightness LaB6 source option
- BeamSleeve option
- Remote Diagnostics over the internet
- Navigation by images from other digital sources
- Improved low kV imaging
- Improved LaB6 imaging for X-ray analysis
- SmartBrowse option for contextual image viewing
- Optibeam modes for high resolution, large depth of field, large field of view and analytics

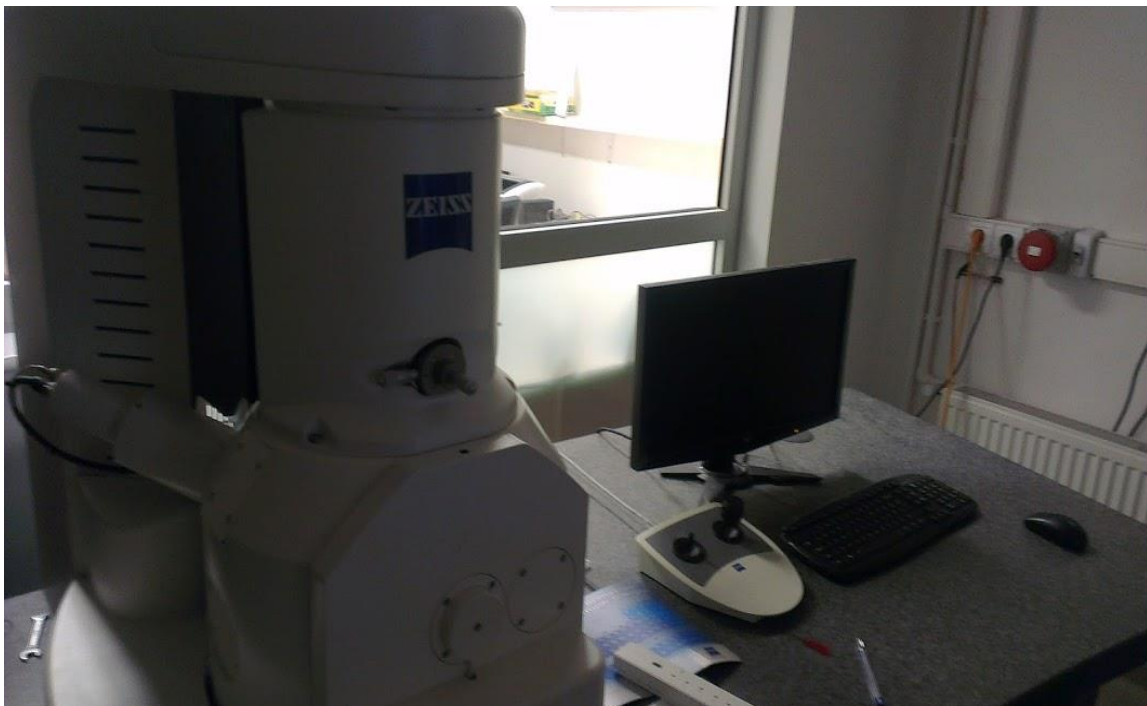


**Figure 3.2 :** Utilized Scanning Electro Spinning (SEM) instrument

### 3.4. Preparation of the Nanofibers by Electrospinning Method

The first electrospinning trials were made using THF and DMF mixture as the solvent to dissolve PU. However, there were difficulties in keeping the solution concentration constant due to high evaporation rate of THF. Also, the fibers obtained by PU and THF solution were not satisfactory, as the fiber diameter was high (above 1 micron). Figure 6 shows the nanofibers obtained by using 45wt% THF and 45wt% DMF 10wt% of the polymer (10gr polyurethane, 45gr DMF, 45gr THF). The voltage was 10 kv, needle-collector distance 15 cm and the flow rate amount 0.5 ml/hr during these trials. The results of the mixed solvent (THF/DMF) showed that the average fiber diameter was 940.32 nm.

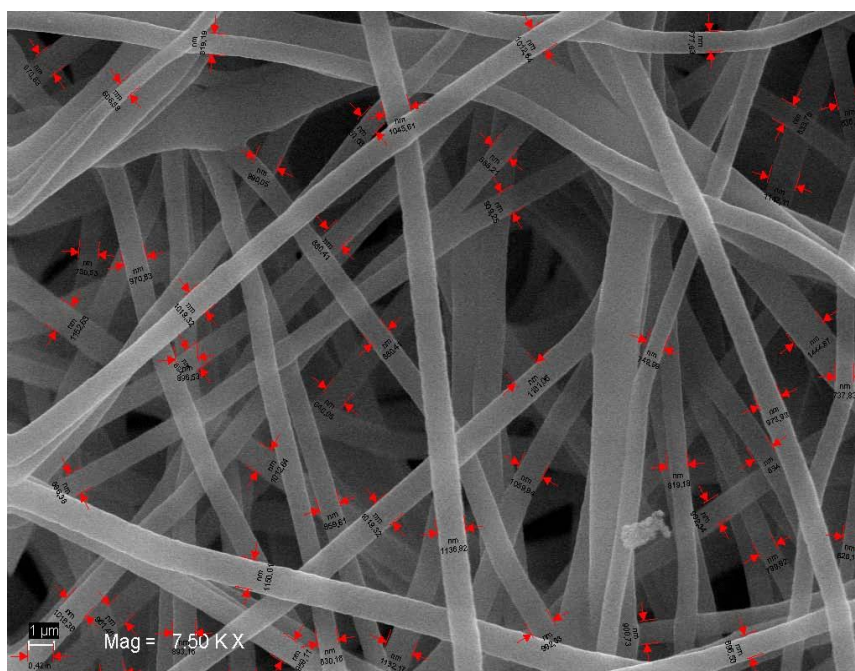


**Figure 3.3 :** SEM Photo and Diameters of Nanofibers Obtained by 10wt% pu , 45wt% THF , 45wt% DMF

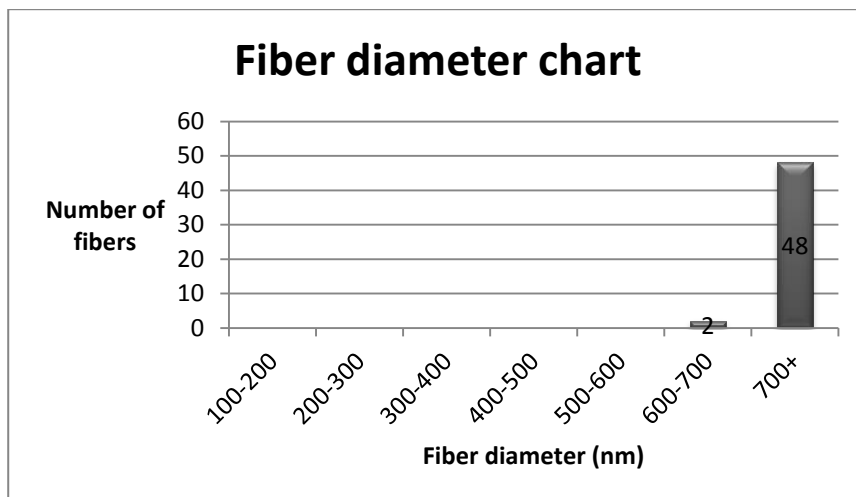


**Figure 3.4 :** Chart of Nanofibers Obtained by 10wt% PU , 45wt% THF , 45wt% DMF

Then trials were made using only DMF as the solvent to dissolve PU. The trials made using DMF as the solvent gave lower nanofiber diameters 156.79 to 621.24nm (Average fiber diameter was 329.57 nm)

Solution concentration is the most important parameter for electrospinning that effect nanofiber properties [Audrey Frenot et al, 2003], [Kerli Tönurist et. All, 2010]. Applied voltage and tip to collector distance and flow rate are among other important electrospinning parameters. In this study, these parameters were changed in order to see their effect on fiber diameter and morphology.

To achieve more accurate results, we made three samples of each concentration, voltage and Nozzle-Collector distance and compared them with each other to ensure that the results are correct and not changed.

**Table 3.4 :** Table of Prepared Samples

Sample	Concentration	Voltage	Tip to collector distance	Flow rate
1	4wt%	15kv	15cm	0,5ml/hr
2	6wt%	15kv	15cm	0,5ml/hr
3	7wt%	15kv	15cm	0,5ml/hr
4	8wt%	15kv	15cm	0,5ml/hr
5	9wt%	15kv	15cm	0,5ml/hr

6	10wt%	15kv	15cm	0,5ml/hr
7	12wt%	15kv	15cm	0,5ml/hr
8	10wt%	10kv	15cm	0,5ml/hr
9	10wt%	15kv	15cm	0,5ml/hr
10	10wt%	20kv	15cm	0,5ml/hr
11	10wt%	15kv	10cm	0,5ml/hr
12	10wt%	15kv	12.5cm	0.5ml/hr
13	10wt%	15kv	15cm	0.5ml/hr
14	10wt%	15kv	17.5cm	0.5ml/hr
15	10wt%	15kv	20cm	0.5ml/hr

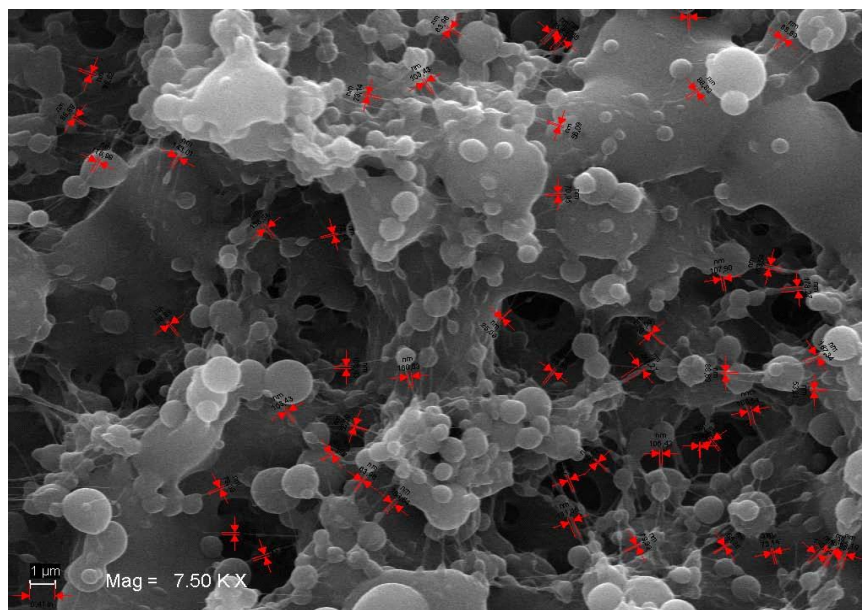


**Figure 3.5 :** 4wt% PU, 15cm Nozzle-Collector Distance, 15KV Applied Voltage, 0.5 ml/hr Polymer Flow Rate

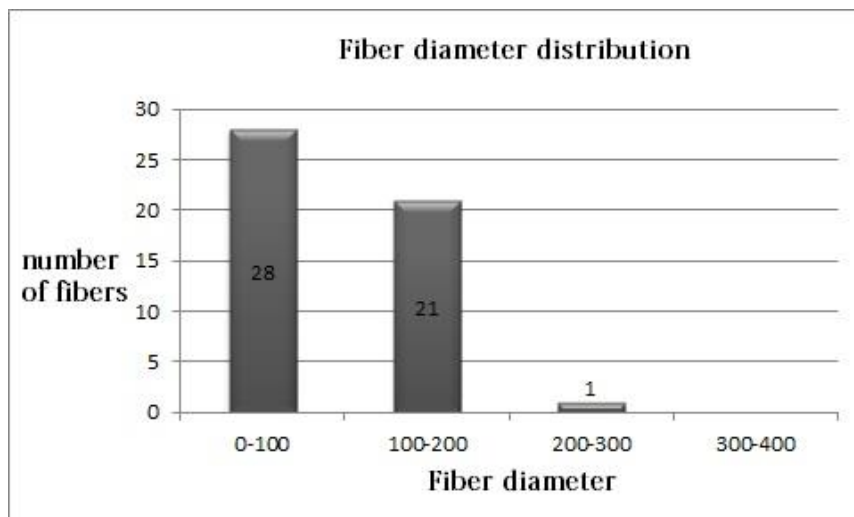


**Figure 3.6 :** 4wt% PU, 15cm Nozzle-Collector Distance, 15KV Applied Voltage, 0.5 ml/hr Polymer Flow Rate

In Figure 7 (4wt% PU) we can see lots of beads and less fibers, despite the fine size of the obtained fibers in this concentration (25-241nm and the Average diameter was 105.08 nm), we cannot call this sample as a nanofiber sample because of the great number of beads and very low number of fibers. In this trial, 4wt% PU/DMF was used as concentration content, the applied voltage was 15kv, the nozzle-collector distance was 15cm and the polymer solution flow rate was 0.5ml/hr (sample 1 in chart 4).

At very low solution concentrations (4 wt%) a large number of sub-micron droplets were present. At such low concentrations, the viscoelastic force (a result of the low degree of chain entanglements) in a given jet segment was not large enough to counter the higher Coulombic force. Therefore, the charged jet was broken into smaller jets and these smaller jets turned into droplets by rounding as a result of the surface tension.

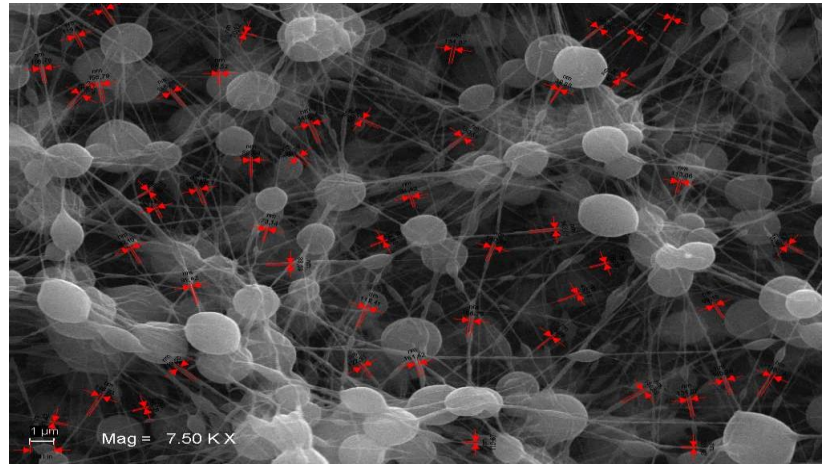


**Figure 3.7 :** 6wt% PU, 15cm Nozzle-Collector Distance, 15KV Applied Voltage, 0.5 ml/hr Polymer Flow Rate

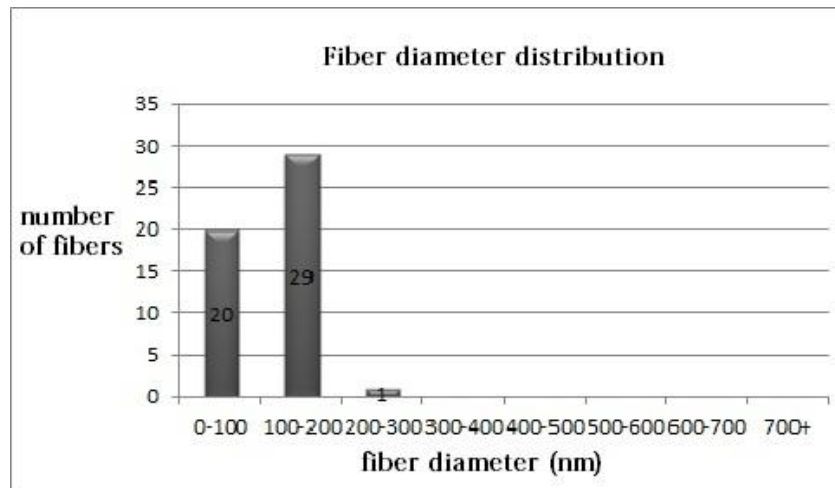


**Figure 3.8 :** 6wt% PU, 15cm Nozzle-Collector Distance, 15KV Applied Voltage, 0.5 ml/hr Polymer Flow Rate

In this trial 6wt% polyurethane/DMF concentration was used, the applied voltage was 15kv, the Nozzle-Collector distance was 15cm and the polymer solution flow rate was 0.5ml/hr. In Figure 8 (6wt% PU) there were more fibers forming comparing with 4wt% sample, although the fibers were fine enough and the number of the fibers increase dramatically with the increase of concentration, still the size and the number of beads are significantly greater than the fibers. The obtained fiber diameters were between 31.36 to 219.5 nm and the average fiber diameter was 114.039 nm (sample 2 in chart 4)



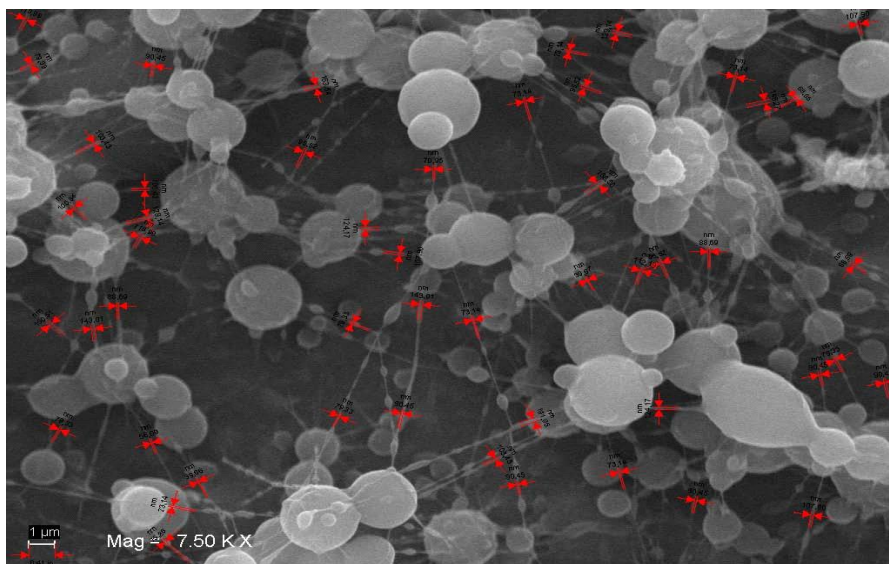


**Figure 3.9 :** SEM Micrograph of Sample 3 (7wt% PU, 15kV, 15cm Distance, 0.5ml/hr flow rate)

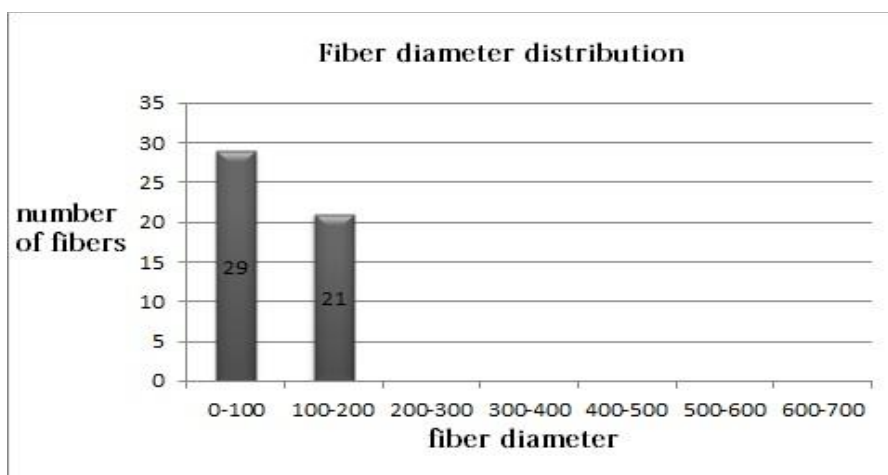


**Figure 3.10 :** Fiber Diameter Distribution of Sample 3 (7wt% PU, 15 kV, 15 cm Distance, 0.5ml/hr Flow Rate)

In this trial the 7wt% PU/DMF concentration was used, the applied voltage was 15kv, the nozzle-collector distance was 15cm and the polymer solution flow rate was 0.5ml/hr (sample 3 in chart4). In this figure (7wt%) we can obviously see that there is still a high number of beads compared to the number of fibers and it is not acceptable. The fibers diameters were between 39.66 nm to 191.05 nm and the average fiber diameter was 99.92 nm.



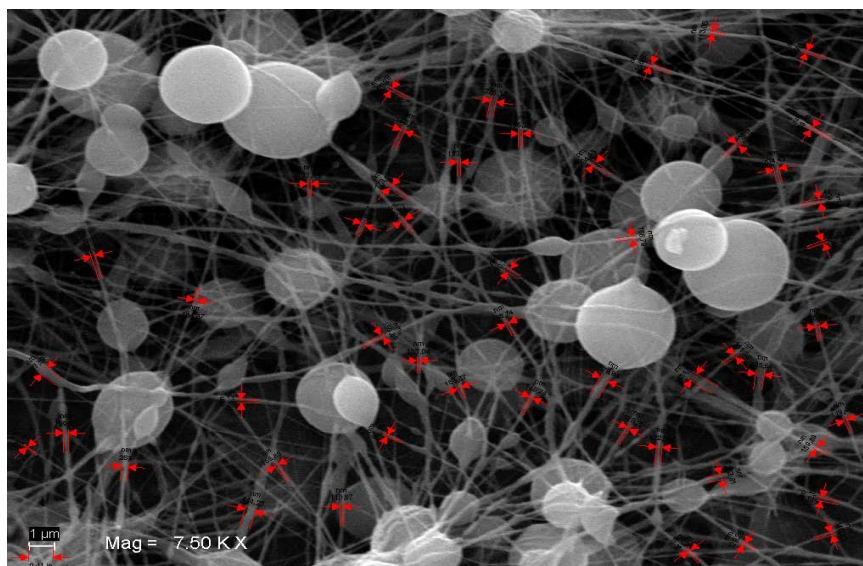


**Figure 3.11 :** SEM Micrograph of Sample 4 (8wt% PU, 15 kV, 15 cm Distance, 0.5ml/hr Flow Rate)

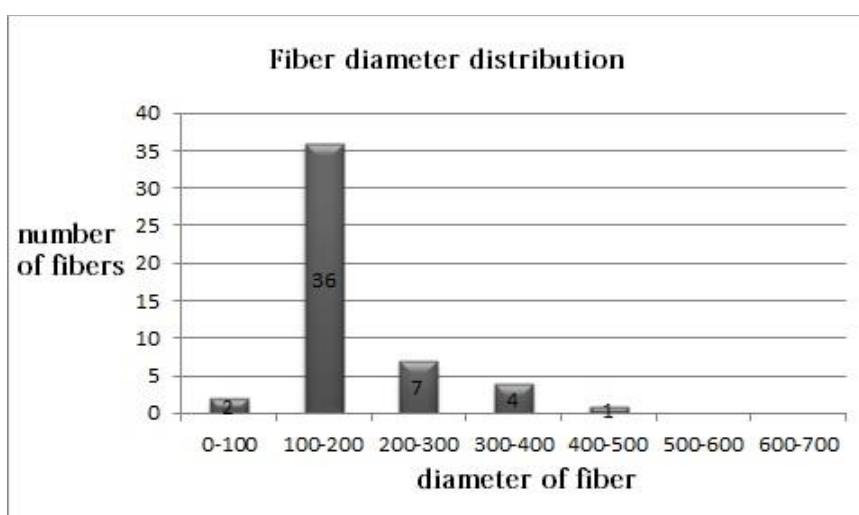


**Figure 3.12 :** Fiber Diameter Distribution of Sample 4 (8wt% PU, 15 kV, 15 cm Distance, 0.5ml/hr Flow Rate)

In this trial the 8wt% PU/DMF concentration was used, the applied voltage was 15kv, the nozzle-collector distance was 15cm and the polymer solution flow rate was 0.5ml/hr (sample 4 in chart3). The average diameter of these trial fibers was 180.99 Nm and the fiber diameter rage was between 62.71 nm to 414.23 nm. Although the fiber diameters are acceptable and fine enough, the number of beads created was still high and due to this high number of beads, this sample was not acceptable.

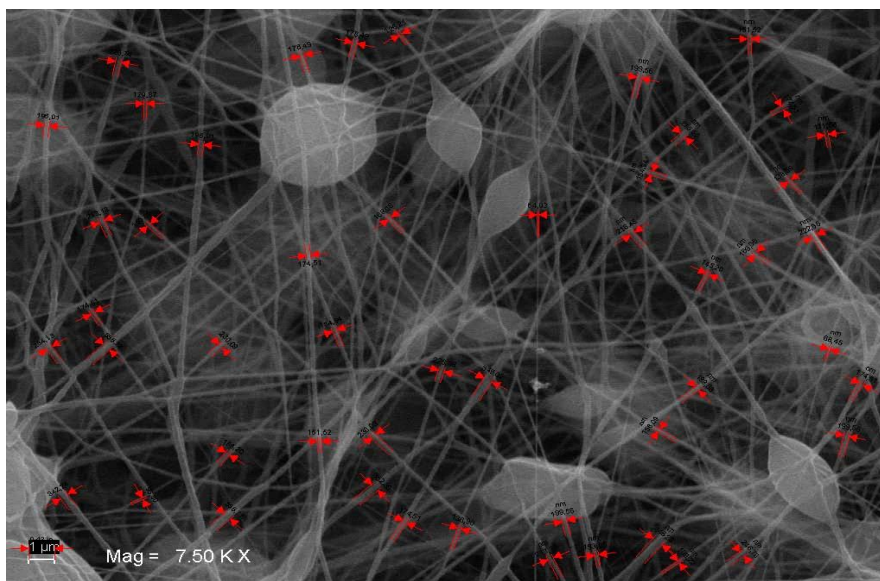


**Figure 3.13 :** SEM Micrograph of Sample 5 (9wt% PU, 15 kV, 15 cm Distance, 0.5ml/hr Flow Rate)

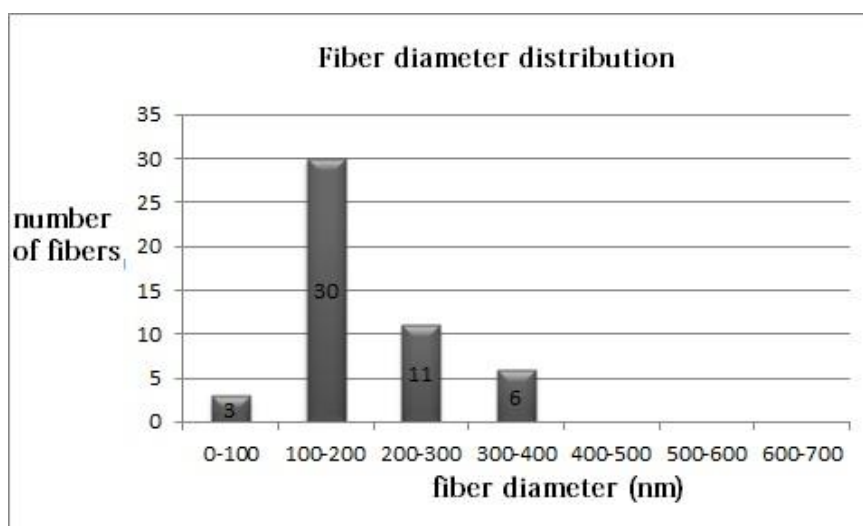


**Figure 3.14 :** Fiber Diameter Distribution of Sample 5 (9wt% PU, 15 kV, 15 cm Distance, 0.5ml/hr Flow Rate)

In this trial the 9wt% PU/DMF concentration was used, the applied voltage was 15kv, the nozzle-collector distance was 15cm and the polymer solution flow rate was 0.5ml/hr (sample 5 in chart3). In this trial fiber diameters were between 64.93 and 446.23nm and the average fiber diameter was 198.36nm.

When high concentrations were used, it was observed that there were nor droplets as the charged jet did not break up into droplets. This could be attributed to the increased chain entanglement and increased viscoelastic force. This suggests that the Coulombic stress elongated the charged jet to the collector. At intermediate

concentrations (6wt%, 7wt%, 8wt%), a combination of nanofibers and droplets was observed. As the concentration was further slightly increased (9wt%), the droplets disappeared and a combination of nanofibers and beaded fibers. The beads had an elongated shape.

In 7, 8, 9 wt% made samples respectively the number of beads were obviously decreased and the number and the diameter of the fibers increased, but still they were not satisfactory because of the beads which still remained even in 9wt% concentration.

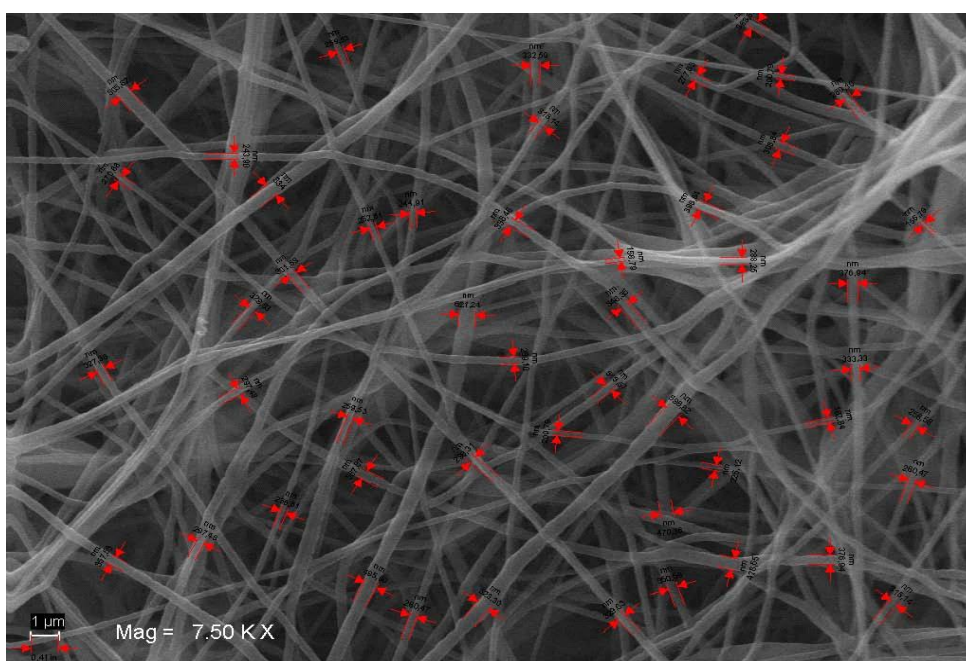


**Figure 3.15 :** 10wt% Sample 6, 15cm Nozzle-Collector Distance, 15kv Applied Voltage, 0.5ml/hr Flow Rate

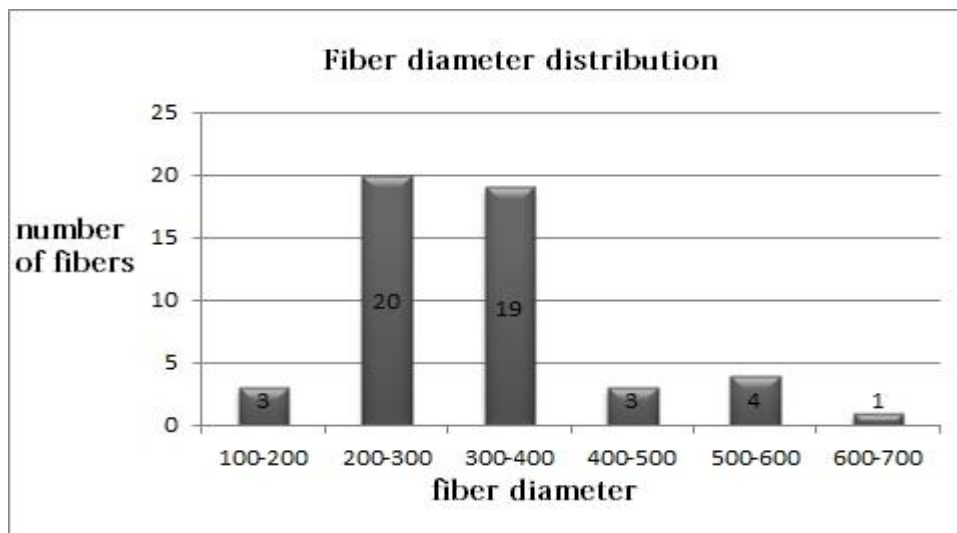


**Figure 3.16 : Sample 6 (10wt% PU) Fiber Diameter Distribution**

In this trial the 10wt% PU/DMF concentration was used, the applied voltage was 15kv, the nozzle-collector distance was 15cm and the polymer solution flow rate was 0.5ml/hr (sample 6 in chart3). The fiber diameters were between 156.79 and 621.24 nm and the average fiber diameter was 329.57 nm. Although this trial had fine enough fibers, no beads appeared, and it was acceptable. Therefore, it was decided to test the 12wt% concentration to observe the characterization results.

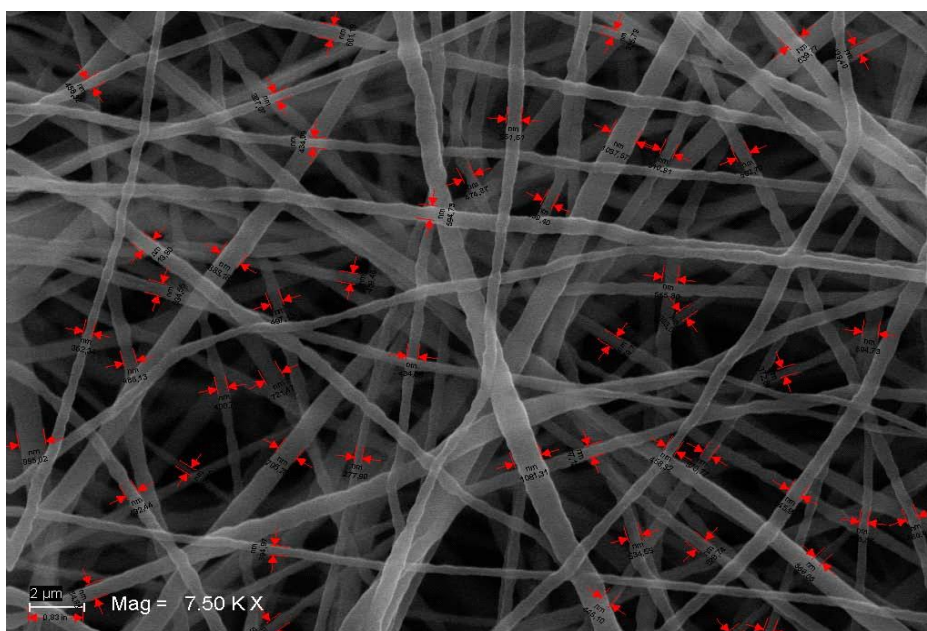


**Figure 3.17 : Sample 7 (12wt% PU) SEM Micrograph**



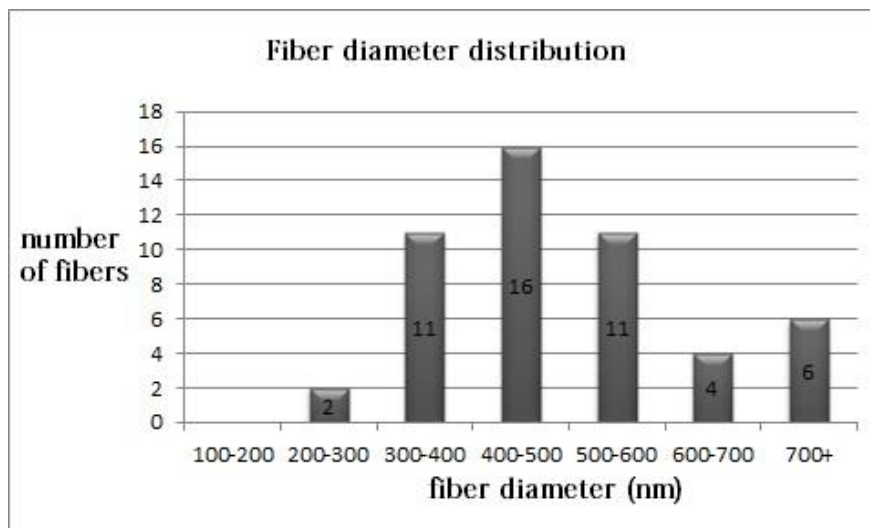


**Figure 3.18 :** Sample 7 (12wt% PU) Fiber Diameter Distribution

In 10wt% concentration sample incredibly the beads almost vanished and the diameter of the fibers were fine enough to be considered as nanofibers (Average 329.57 nm). In 12wt% sample although there were no beads in the fibers structure and the diameters of the fibers were still fine enough (Average 519.60 nm), the diameters of the fibers which had been produced with 10wt% concentration were better due to their delicacy.

After the determination of the best concentration, the other parameters (nozzle-collector distance, applying voltage and the solution flow rate) were individually examined.



**Figure 3.19 :** Nozzle-Collector Distance

When the determination of the most appropriate solution concentration, which is the most important factor between the other parameters, was done, the nozzle-collector

distance examination started. For this purpose, samples with 10, 12.5, 15, 17.5, 20 Cm nozzle-collector distances were subjected for an hour to the electrospinning model and the SEM photographs of each sample was taken and the morphology of the fibers investigated. In this study, other parameters of the electrospinning process were constant (10wt% concentration, 0.5 ml/hr feeding rate, 15 KV electrical supply). A SEM photograph of each sample is shown in Figures 14 to 18.

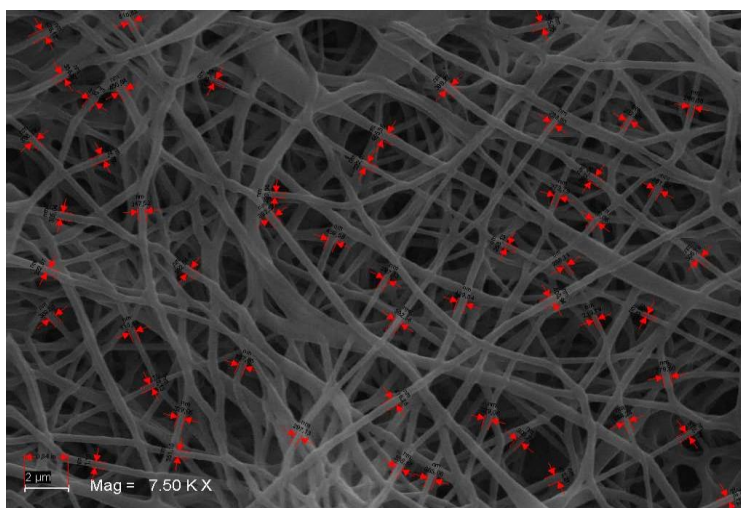


**Figure 3.20 :** SEM Micrographs of Sample 8 (10cm Nozzle-Collector Distance, 15kv Supplied Voltage, 10wt% Solution Concentration, 0.5ml/hr Flow Rate)

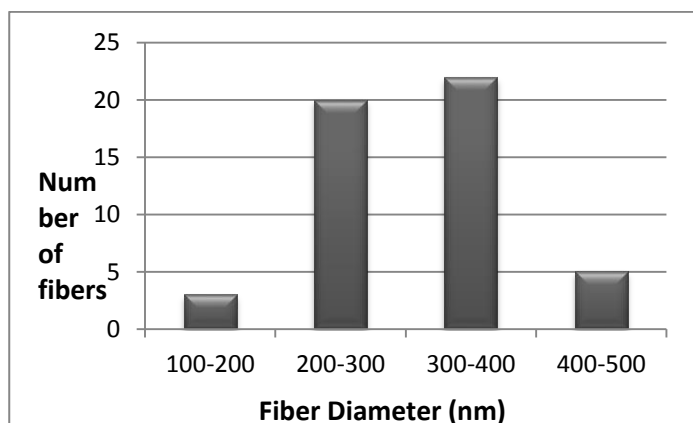


**Figure 3.21 :** Fiber Diameter Distribution of Sample 8 (10cm Nozzle-Collector Distance, 15kv Supplied Voltage, 10wt% Solution Concentration, 0.5ml/hr Flow Rate)

In this trial (figure 14), the 10wt% PU/DMF concentration was used as the polymer solution, 15kv electric field applied, and the solution flow rate was 0.5 ml/hr, but at this time the Nozzle-collector distance was 10cm (sample 11 in chart 3). As you can see in the figure 14, there is no bead between the fibers, but the diameter of the fibers

is approximately high (between 193.6nm and 465.36nm), so we decided to increase the nozzle-collector distance to achieve finer diameters.

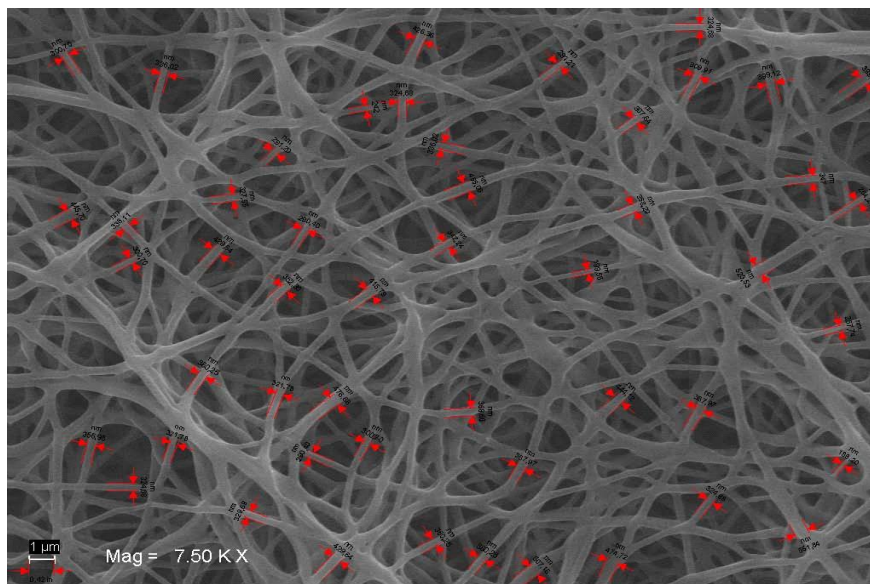


**Figure 3.22 :** SEM Micrographs of Sample 9 (12.5cm Nozzle-Collector Distance, 15kv Supplied Voltage, 10wt% Solution Concentration, 0.5ml/hr Flow Rate)

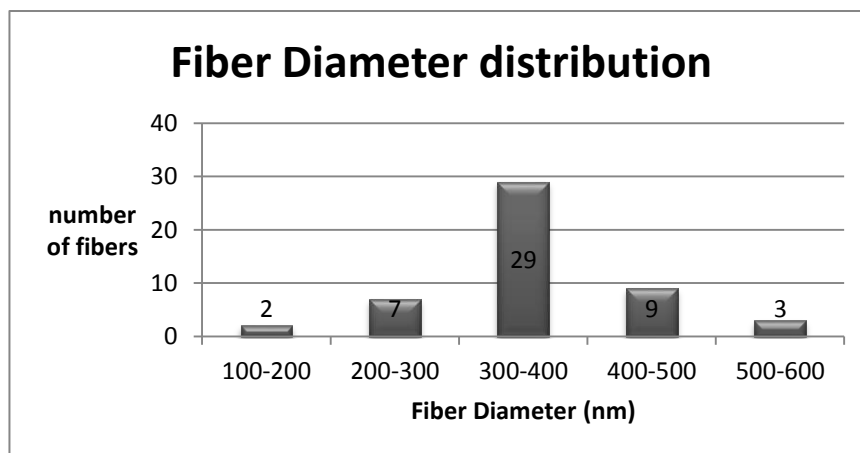


**Figure 3.23 :** Fiber Diameter Distribution of Sample 9 (12.5cm nozzle-collector Distance, 15kv Supplied Voltage, 10wt% Solution Concentration, 0.5ml/hr Flow Rate)

In this trial (figure 15), the 10wt% PU/DMF concentration was used as the polymer solution, 15kv electric field applied, and the solution flow rate was 0.5 ml/hr, but at this time the Nozzle-collector distance was 12.5cm (sample 12 in chart 3). The average fiber diameter in this trial was 355.45 nm and the diameters were between 186.2 nm and 551.84 nm.

Comparing 10cm to 12.5cm Nozzle-Collector distance SEM results (Figure14 and Figure 15), we can observe that the fiber diameters are decreasing slightly with the increase in the Nozzle-Collector distance. This is also in accordance with the findings in the literature. The longer path length between the nozzle tip and the collector means that there will be a higher probability for the jet segment to thin down as a result of the Coulombic repulsion [Mit-uppatham et al., 2004].

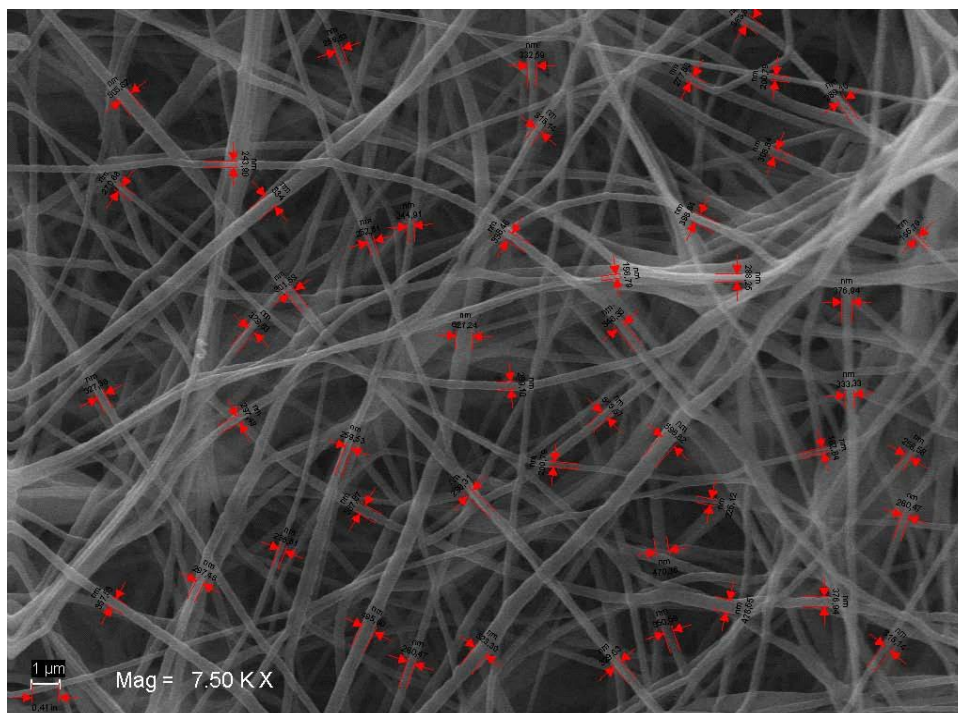


**Figure 3.24 :** SEM Micrograph of Sample 10 (15cm Nozzle-Collector Distance, 15kv Supplied Voltage, 10wt% Solution Concentration, 0.5ml/hr Flow Rate)

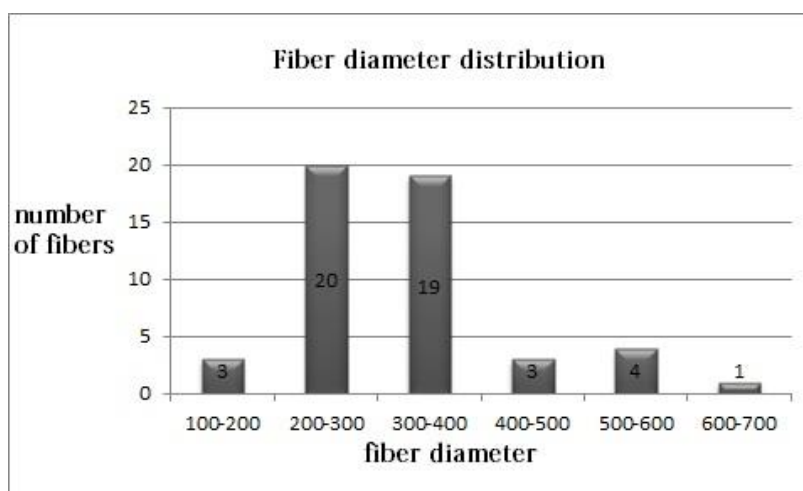


**Figure 3.25 :** Fiber Diameter Distribution of Sample 10



In this trial (figure 16), the 10wt% PU/DMF concentration was used as the polymer solution, 15kv electric field applied, and the solution flow rate was 0.5 ml/hr, but at this time the Nozzle-collector distance was 15cm (sample 13 in chart 3).The fiber diameters were between 156.79 and 621.24 nm and the average fiber diameter was 329.57 nm.

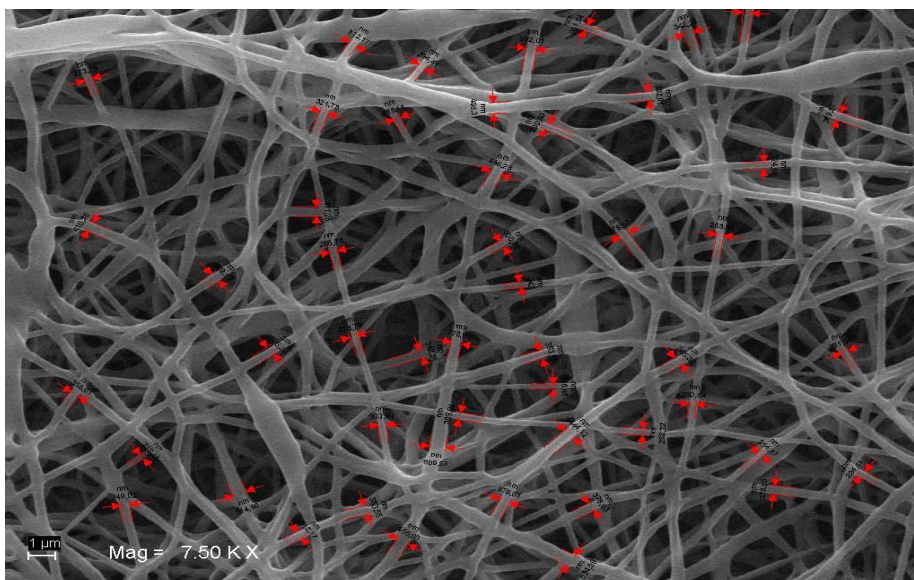


**Figure 3.26 :** SEM Micrograph of Sample 11 (17.5cm Nozzle-Collector Distance, 15kv Supplied Voltage, 10wt% Solution Concentration, 0.5ml/hr Flow Rate)

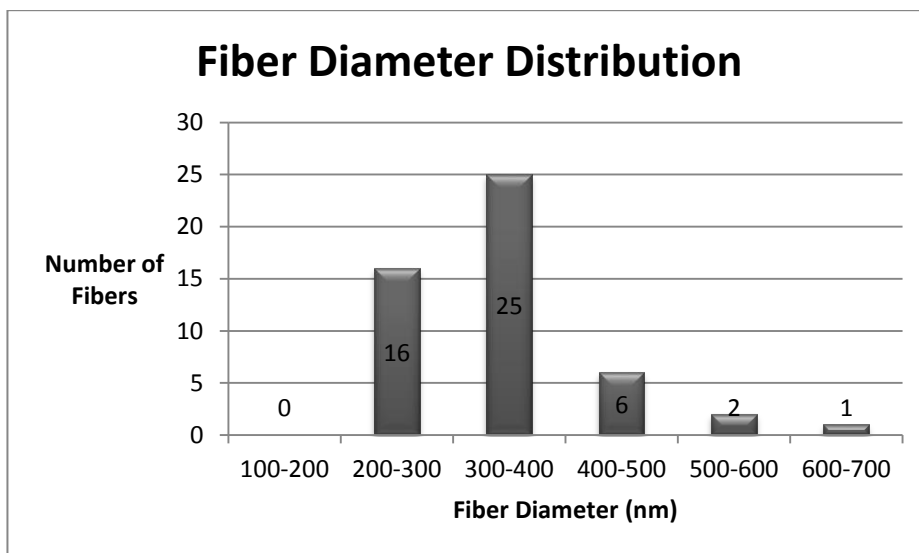


**Figure 3.27 :** Fiber Diameter Distribution of Sample 11

In this trial (figure 17), the 10wt% PU/DMF concentration was used as the polymer solution, 15kv electric field applied, and the solution flow rate was 0.5 ml/hr, but at this time the Nozzle-collector distance was 17.5cm (sample 14 in chart 3).The fiber

diameters were between 214.27 and 609.53 nm and the average fiber diameter was 347.01 nm.

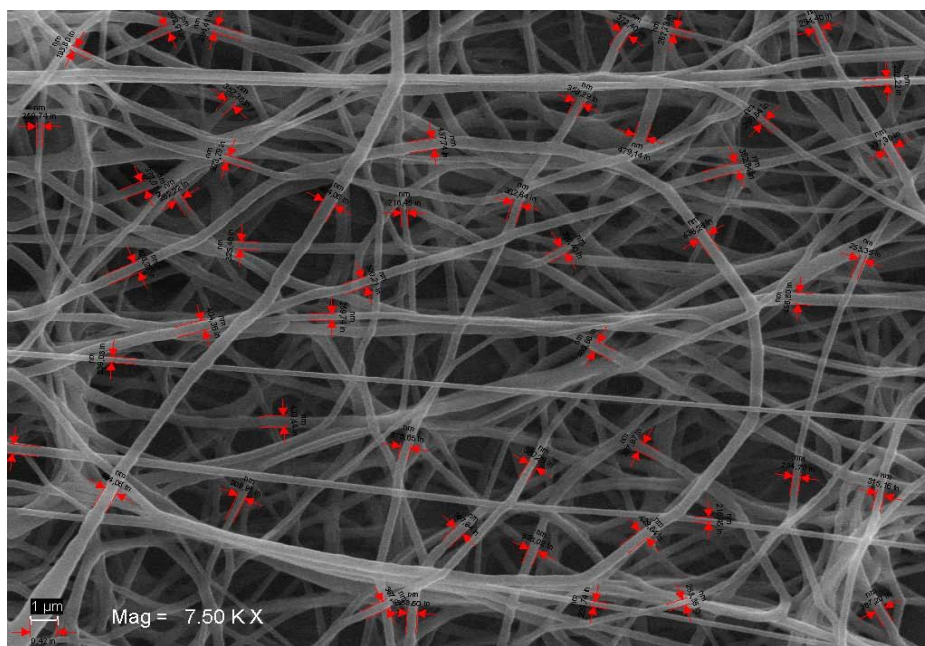


**Figure 3.28 :** SEM Micrograph of Sample 12 (20cm Nozzle-Collector Distance, 15kv Supplied Voltage, 10wt% Solution Concentration, 0.5ml/hr Flow Rate)

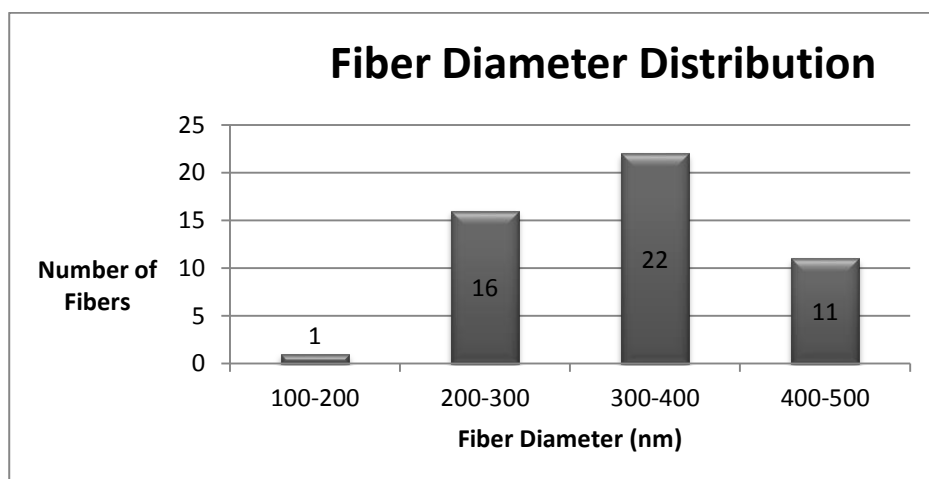


**Figure 3.29 :** Fiber Diameter Distribution of Sample 12 (20cm nozzle-collector Distance, 15kv Supplied Voltage, 10wt% Solution Concentration, 0.5ml/hr Flow Rate)

In this trial (figure 18), the 10wt% PU/DMF concentration was used as the polymer solution, 15kv electric field applied, and the solution flow rate was 0.5 ml/hr, but at this time the nozzle-collector distance was 20cm (sample 15 in chart 3). The fiber

diameters were between 193.6 nm and 494.6 nm and the average fiber diameter was 344.23 nm.

Perusing the remaining SEM results (Figures 16, 17, 18), respectively, there is a slight decrease in fibers diameter with an increase in nozzle-collector distance, there is also an increase in the number of existing beads. Formation of beads is an unpleasant behavior and minimizing the beads number is one of our goals, to achieve homogeneous products. In this study, the 15cm nozzle-collector distance sample gained the best result between the others, because it has the finest fiber diameters between the other samples which had less nozzle-collector distances, and less beads comparing with the samples which had more nozzle-collector distances.



**Figure 3.30 :** Utilized DC High Electrical Voltage Supplier

The electric field which applied to the polymers, produced by a DC high electrical voltage supplier, with an adjustable voltage switch, so we had chance to study on the fibers behavior in constant situation and different voltage supply, in this study, three different voltages applied on each polymer sample, in a constant situations (15cm Nozzle-Collector distance, 10wt% PU solution, 0.5 ml/hr feeding rate, 25 °C, 1 atm) subjected for an hour under the electrospinning model, SEM photographs of each sample was taken, and the morphology of the fibers investigated. The SEM results of each sample are shown in Figures 19, 20, 21.

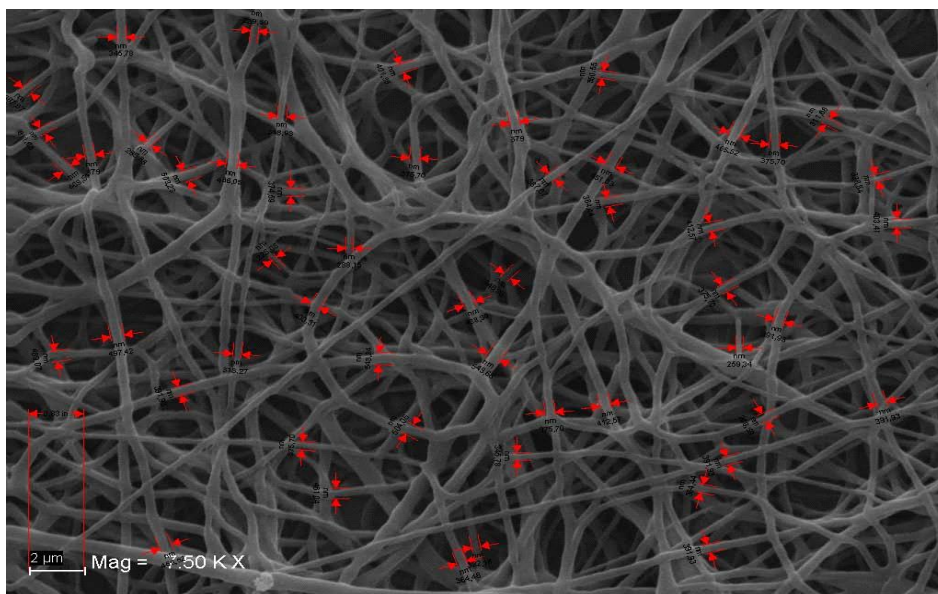


**Figure 3.31 :** Sample 13, 10kv Applied, 10wt% PU, 15cm Distance, 0.5ml/hr Flow Rate

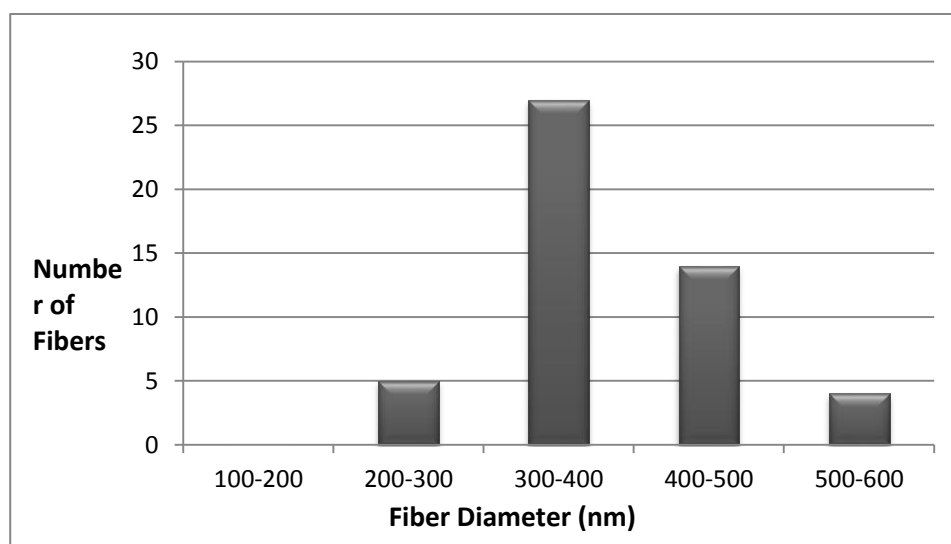


**Figure 3.32 :** Sample 13, 10kv Applied, 10wt% PU, 15cm Distance, 0.5ml/hr Flow Rate

In this trial, we used 10wt% PU/DMF solution concentration, 15cm Nozzle-Collector distance, 0.5ml/hr solution flow rate, but we changed the applied voltage to 10KV to determine the best electrical field for electrospinning the used polyurethane.

The achieved fibers in this study had diameters between 225.05 nm and 548.24 nm , and the average fiber diameter was 391.64 nm.



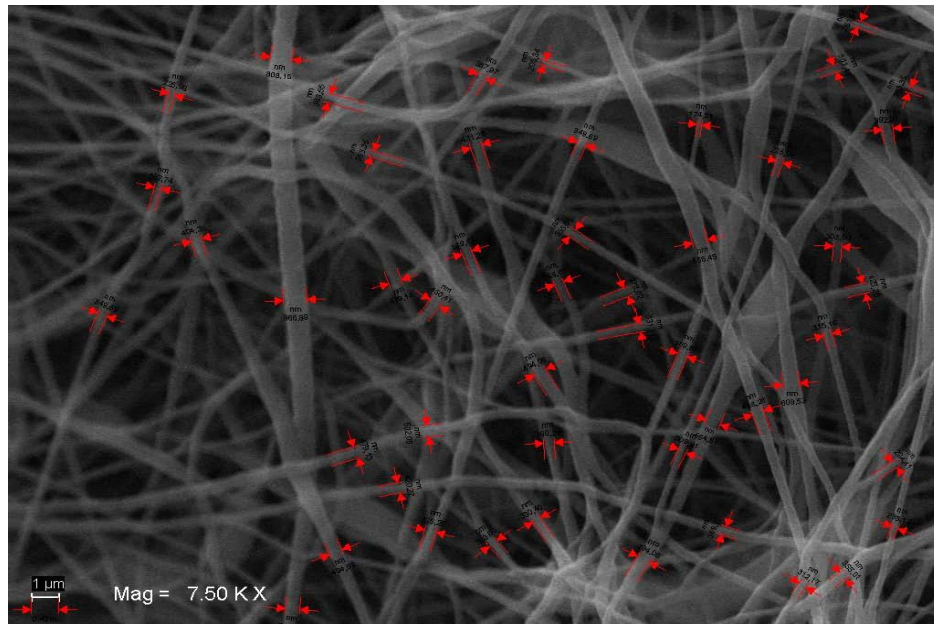


**Figure 3.33 :** Sample 14, 15kv Applied, 10wt% PU, 15cm Distance, 0.5ml/hr Flow Rate

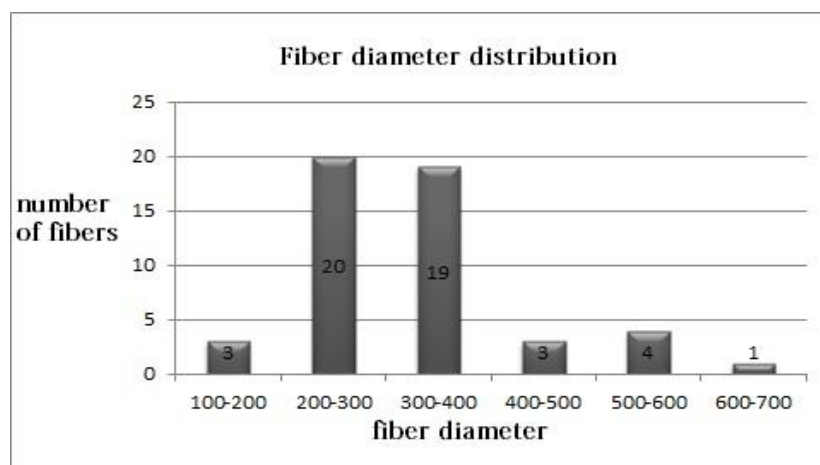


**Figure 3.34 :** Sample 14, 15kv Applied, 10wt% PU, 15cm Distance, 0.5ml/hr Flow Rate

In this trial, we used 10wt% PU/DMF solution concentration, 15cm Nozzle-Collector distance, 0.5ml/hr solution flow rate, but we changed the applied voltage to 15KV to determine the best electrical field for electrospinning the used polyurethane.

The achieved fibers in this study had diameters between 174.51 nm and 866.89nm , and the average fiber diameter was 391.07 nm.

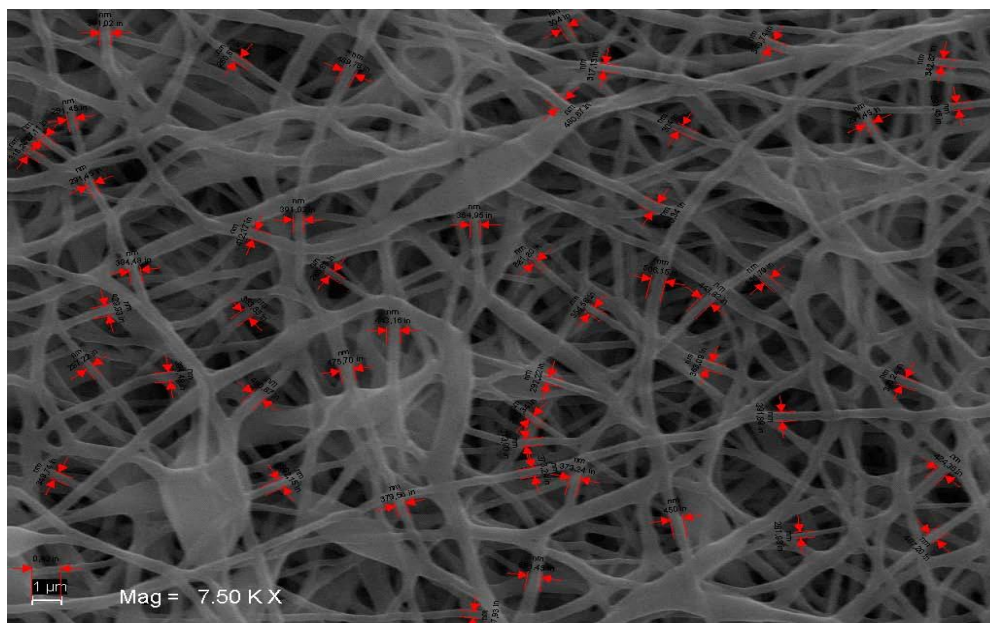


**Figure 3.35 :** Sample 15, 20kv Applied, 15kv Applied, 10wt% PU, 15cm Distance, 0.5ml/hr Flow Rate

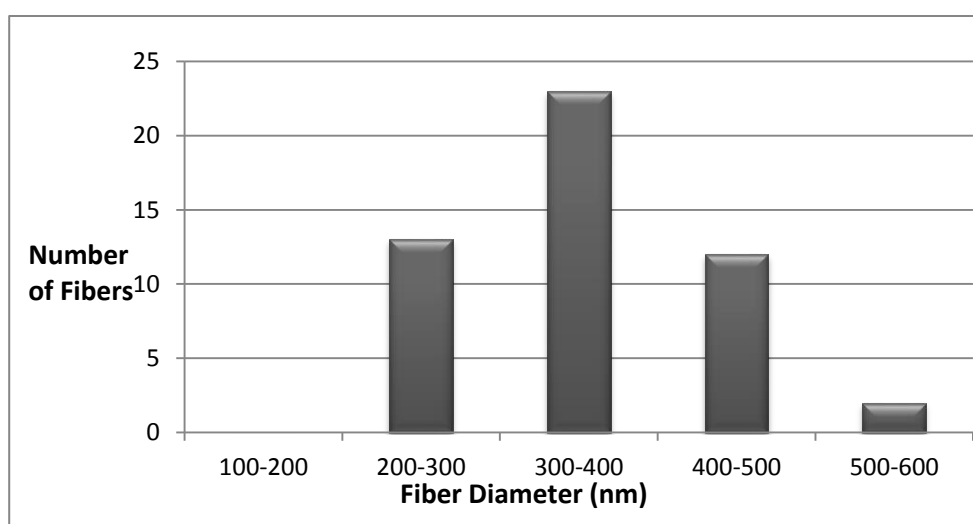


**Figure 3.36 :** Sample 15, 20kv Applied, 15kv Applied, 10wt% PU, 15cm Distance, 0.5ml/hr Flow Rate

In this trial, 10wt% PU/DMF solution concentration, 15cm Nozzle-Collector distance and 0.5ml/hr solution flow rate was used, but we changed the applied voltage to 20KV to determine the best electrical field for electrospinning the utilized polyurethane.

The achieved fibers in this study had diameters among 221.2 nm and 506.15 nm, and the average fiber diameter was 364.48 nm.

Comparing Figure19 to Figure 20 (10KV vs. 15KV samples), an increase in applied voltage causes a slight decrease in fiber diameters and still no beads observed (391.64 – 391.07 nm). With an increase in applied voltage up to 20KV in third sample (Figure 21) the fiber diameters still were decreasing (The average fiber diameter was 364.48 nm) but the formation of beads started, so, due to our aim which was to achieve finest fibers with less or no beads,we decided that, the most appropriate voltage would be 15KV.

## **4. CONCLUSIONS AND RECOMMENDATIONS**

### **4.1. Results and Conclusions:**

In this study different samples, with different polymer concentrations, voltages and nozzle-Collector distances were made, so we had to determinate the best ones between the others, to determinate the best concentration between 4wt%, 6wt%, 7wt%, 8wt%, 9wt%, 10wt% and 12wt% polymer concentrations, each concentration was investigated carefully:

In Figure 7 (4wt% PU) we can see lots of Beads and less fibers, despite the fine size of the obtained fibers in this concentration (105.08 nm), we cannot call this sample a Nanofiber sample because of the great number of beads.

In Figure 8 (6wt% PU) there were more fibers forming comparing with 4wt% sample, although the fibers were fine enough (114.03 nm) and the number of the fibers were increasing dramatically with the increase of concentration, still the size and the number of beads are significantly greater than the fibers.

In 7, 8, 9 wt% made samples respectively the number of beads were obviously decreasing and the number and the diameter of the fibers were increasing (99.92, 180.99, 198.36 nm), but still they were not satisfactory because of the beads which still were remaining even in 9wt% concentration.

In 10wt% concentration sample incredibly the beads were almost vanished and the diameter of the fibers were fine enough to be considered as nanofibers (329.57 nm). In 12wt% sample although there were no beads in the fibers structure and the diameters of the fibers were still fine enough (519.60 nm), the diameters of the fibers which had been produced with 10wt% concentration were better due to their delicacy.

After the determination of the best concentration, the other parameters (nozzle-collector distance, applying voltage and the solution feeding rate) were examined Individually.



To determinate the best Nozzle-Collector distance between the samples, which were made with different distances (10cm, 12.5cm, 15cm, 17.5cm, 20cm), each sample was investigated carefully.

Comparing 10cm to 12.5cm nozzle-collector distance SEM results (Figure14 and Figure 15), we can observe that the fiber diameters are decreasing slightly with the increase of the nozzle-collector distance, and the number of beads are increasing with the increase of the nozzle-collector distance.

Perusing the remaining SEM results (Figures 16, 17, 18), respectively, there is a slight decrease in fibers diameter with an increase in nozzle-collector distance, there is also an increase in the number of existing beads, which is increasing when the Nozzle-Collector distance rises. Formation of the beads is an unpleasant behavior, and minimizing the beads number is one of our goals to achieve homogeneous products. In this study, the 15cm nozzle-collector distance sample gained the best result between the others, because it has the finest fiber diameters between the samples which had less nozzle-collector distances and less beads comparing with the samples which had more nozzle-collector distances.

To determinate the best Voltage applied between the samples which were made with different voltages (10kv, 15kv, 20kv), each sample was investigated carefully.

Comparing Figure19 to Figure 20 (10KV vs. 15KV samples), an increase in applied voltage causes a slight decrease in fiber diameters and still no beads observed (391.64 –391.07 nm). With an increase in applied voltage up to 20KV in third sample (Figure 21) the fiber diameters still were decreasing (364.48 nm) but the formation of beads started, our aim is to achieve finest fibers with less or no beads so the most appropriate voltage would be 15KV.

Briefly, the best nanofiber we obtained in this study was made by 10wt% (PU/DMF) solution concentration, 15KV electric supply, 15cm Nozzle-collector distance and 0.5ml/hr polymer flow rate.

## REFERENCES

- A. Formhals**, US Patent 1,975,504 (1934), inv
- A. Formhals**, US Patent 2,349,950 (1944), inv.
- Adomaviciute E, Milasius Rimvydas**. The influence of applied voltage on poly (vinyl alcohol) (PVA) nanofibre diameter. *Fibers Text East Eur* 2007;15:64–5.
- Audrey Frenot, IoannisS. Chronakis** - *IFP Research, Swedish Institute for Fiber and Polymer Research, P.O. Box 104, S-431 22 Mölndal, Sweden* 2003.
- Bhardwaj, N., Kundu, S. C.** Electrospinning: A Fascinating Fiber Fabrication Technique *Biotechnology Advances* 28 - 2010: pp. 325 – 347.
- Bumsu Kim, Hyun Park, Sung-Hwan Lee, Wolfgang M. Sigmund**, Department of Materials Science and Engineering, University of Florida, 2004
- C.J. Thompson, G.G. Case, A.L. Yarin and D.H. Reneker**, "Effects of Parameters on Nanofiber Diameter Determined from Electrospinning Model", *Nanotechnology Research: New Nanostructures*. (Xiaohua Huang, Ed.). Chapter 6, pp. 223-242, Nova Science Publishers Inc., 2007.
- Cengiz, F., Jirsak, O.** The Effect of Salt on the Roller Electrospinning of Polyurethane Nanofibers, *Fibers and Polymers* 10 (2) 2009: pp. 177 – 184.
- Cha, D. I., Kim, H. Y., Lee, K. H., Jung, Y. Ch., Cho, J. W., Chun, B. Ch.** Electrospun Nonwovens of Shape- Memory Polyurethane Block Copolymers *Polymer Science* 96 2005: pp. 460 – 465.
- Chen, M., Zho, D.-L., Chen, Y., Zhu, P.-X.** Analyses of Structures for a Synthetic Leather Made of Polyurethane and Microfiber *Polymer Science* 103 2007: pp. 903 – 908.
- Chidchanok Mit-uppatham, Manit Nithitanakul, Pitt Supaphol**, The Petroleum and Petrochemical College, Chulalongkorn University, 2004.
- Cungang-ro, Anseong-si, - Gyeonggi-do, Jun-Seo Park** - Division of Chemical Engineering, Hankyong National University, 167 456-749, Korea, Electrospinning and its applications, 2011
- D. H. Reneker, A. L. Yarin, H. Fong, S. Koombhongse, J.** *Appl. Phys.* Electrospun Gelatin Fibers, 2000, 87, 4531.
- D. H. Reneker, I. Chun**, *Nanotechnology* 1996, 7, 216.
- D. Jakšić**: Possibilities of Determining Porosity of Textile Fabrics, *Tekstilec*, 37 (7-8) 221- 228 (1994.)

- Deitzel JM, Kleinmeyer J, Hirvonen JK, BeckTNC.** Controlled Deposition of Electrospun poly(ethylene oxide) fibers. *Polymer* 2001;42:8163–70.
- Deitzel, J.M., Kleinmeyer, J., Harris, D., and Tan, N.C.B.** The effect of processing variables on the morphology of electrospun nanofibers and textiles 2001
- Doshi, J., and Reneker, D.H.** Electrospinning process and applications of electrospun fibers. *J. Electrostat.* 35, 151, 1995.
- E. Zdraveva, N. Pejnovic, B. Mijovic** - *University of Zagreb, Faculty of Textile Technology*, Electrospinning Of Polyurethane Nonwoven Fibrous Mats.
- Feng L, Li S, Li H, Zhai J, Song Y, Jiang L, et al.** SuperHydrophobic Surface of Aligned Polyacrylonitrile Nanofibers. *Angew Chem Int Ed* 2002;41(7):1221–3.
- Fong H, Reneker DH.** Electrospinning and formation of nano- fibers. In: Salem DR, editor. *Structure formation in polymeric fibers*. Munich: Hanser; 2001. p. 225–46.
- Han, J., Chen, B., Ye, L., Zhang, A., Zhang, J., Feng, Z.** - Synthesis and Characterization of Biodegradable Polyurethane Based on Poly( $\epsilon$ -caprolactone) and L-lysine Ethyl Ester Diisocyanate *Frontiers of Materials Science* - 3 (1) 2009: pp. 25 – 32.
- Heikkila P and Harlin A,** Parameter study of electro-spinning of polyamide-6, *Euro. Polym. J.*, 44(10), 3067- 3079, 2008.
- Huang ZM, Zhang YZ, Kotaki M, Ramakrishna S.** A review on polymer nanofibers by electrospinning and their applications in nanocomposites. *Compos Sci Technol* 2003;63:2223–53
- Huceste Catalgil Giz, Ahmet Giz, Wayne F. Reed. Macro,** Novel methods for characterizing polyelectrolyte synthesis and solution properties, 2006.
- J. Cross,** “Electrostatics: Principles, Problems, and Applications”, Adam Hilger, Bristol 1987.
- J. Doshi, D. H. Reneker, J.** Electrostatics. 1995, 35, 151.
- J.P. Theron, J.H. Knoetze, R.D. Sanderson, R. Hunter, K. Mequanint, T. Franz, P. Zilla, D. Bezuidenhout.** Modification, crosslinking and reactive electrospinning of a thermoplastic medical polyurethane for vascular graft applications, 2010
- Jamil A. Matthews, Gary E. Wnek, David G. Simpson, and Gary L. Bowlin** Electrospinning of collagen nanofibers, 2001
- Jia Y T, Gong J, Gu X H, Kim H Y, Dong J and Shen X Y** 2007 - *Carbohydr. Polym.* 67 403
- Kang, Y. K., Park, C. H., Kim, J., Kang, T. J.** Application of Electrospun Polyurethane Web to Breathable Water-proof Fabrics *Fibers and Polymers* 8 (5) 2007: pp. 564 – 570.

- Kerli Tõnurist, Thomas Thomberg, Tavo Romann, Enn Lust** Institute of Chemistry, University of Tartu, Estonia, Influence Of Electrospinning Parameters..., 2009.
- Kidoaki S, Kwon IK, Matsuda T.** Mesoscopic spatial designs of nano and microfiber meshes for tissue-engineering matrix and scaffold based on newly devised multilayering and mixing electrospinning techniques. *Biomaterials* 2005;26:37–46.
- Kristine Graham, Ming Ouyang, Tom Raether, Tim Grafe, Bruce McDonald, Paul Knauf** Donaldson Co., Inc., PO Box 1299, Minneapolis, MN 55440, 2002
- L.Wannatong, A. Sirivat, P. Supaphol,** *Polym.Int.* 2004, 53, 1851.
- Leon M. Bellan and Harold G. Craighead** , Applications of controlled electrospinning Systems - 2010
- Liang D, Hsiao BS, Chu B.** Functional electrospun nanofibrous scaffolds for biomedical applications. *Adv Drug Deliv Rev* 2007;59:1392–412.
- Liu GJ, Ding JF, Qiao LJ, Guo A, Dymov BP, Gleeson JT, et al.** Polystyrene-block-poly (2-cinnamoyl ethyl methacrylate) nanofibers-Preparation, characterization, and liquid crystalline properties. *Chem-A European J* 1999;5:2740–9.
- M.M. Demir , I. Yilgor , E. Yilgor , B. Erman** – Faculty of engineering and natural science , Sabanci university , orhanli , 81474 , Tuzla , Istanbul , Turkey 2002
- Ma PX, Zhang R.** Synthetic nano-scale fibrous extracellular matrix. *J Biomed Mat Res* 1999;46:60–72.
- Mark Aronoff and Kirsten Fudeman,** what is morphology, 2010.
- Martin CR.** Membrane-based synthesis of nanomaterials. *Chem Mater* 1996;8:1739–4.
- Mengyan Li, Mark J. Mondrinos, Milind R. Gandhi, Frank K. Ko, Anthony S. Weiss, Peter I. Lekes** 2005
- Mengyan Li, Mark J. Mondrinos, Milind R. Gandhi, Frank K. Ko, Anthony S. Weiss, Peter I. Lekes** 2004
- Mondal S.** 2008 *Appl. Therm. Eng.* 28 1536
- Ondarcuhu T, Joachim C.** Drawing a single nanofibre over hundreds of microns. *Europhys Lett* 1998;42(2):215–20.
- P. Durst:** PU Transfer Coating of Fabrics for Leather like Fashion Products, *Journal of Coated Fabrics*, 14, 227-241 (1985.)
- P. K. Baumgarten, J.** *Colloid Interface Sci.* 1971, 36, 71.
- Pedicini, A., Farris, R. J.** Mechanical Behavior of Electrospun Polyurethane Polymer 2003 44 pp. 6857 – 6862.
- Phillip W. Gibson, Ph.D., Calvin Lee, Ph.D., Frank Ko, Ph.D. Darrell Reneker, Ph.D.**
- Quynh P. Pham, Upma Sharma, Ph.D., And Antonios G. Mikos, Ph.D.** 2006

- Rockwood, D. N., Akins, R. E. Jr., Parrag, I. C., Woodhouse, K. A., Rabolt, J. F.** Culture on Electrospun polyurethane Scaffolds Decreases Atrial Natriuretic Peptide Expression by Cardiomyocytes in Vitro *Biomaterials* 29 - 2008: pp. 4783 – 4791.
- S. R. Singh**, Principles of Optical and Electron Microscopy, National Metallurgical Laboratory, Jamshedpur - 831 007.
- Sanders, J. E., Bale, S. D., Neumann, T.** Tissue Response to Microfibers of Different Polymers: Polyester, Polyethylene, Polylactic Acid, and Polyurethane *Biomedical Materials* 62 2002: pp. 222 – 227.
- Sheikh, F. A., Barakat, N. A. M., Kanjwal, M. A., Chaudhari, A. A., Jung, I.-H., Lee, J. H., Kim, H. Y.** Electrospun Antimicrobial Polyurethane Nanofibers Containing Silver Nanoparticles for Biotechnological - Applications *Macromolecular Research* 17(9) 2009: - pp. 688 – 696.
- Sill TJ, Recum HAV.** Electrospinning: applications in drug delivery and tissue engineering. *Biomaterials* 2008;29:1989–2006.
- Stana Kovačević, Darko Ujević and Snježana Brnada** , University of Zagreb Faculty of Textile Technology Department of Textile Design and Management ,Department of Clothing Technology Baruna Filipovića 28a, 10000 Zagreb, Croatia
- Stankus JJ, Guan J, Wagner WR.** Fabrication of biodegradable elastomeric scaffolds with sub-micron morphologies. *J Biomed Mater Res* 2004;70A:603–14.
- Taylor GI.** Electrically Driven Jets. *Proc R Soc Lond, A Math Phys Sci*, (1934–1990), 1969; 313, 453-75. 2011.
- Thandavamoorthy Subbiah, G. S. Bhat, R. W. Tock, S. Parameswaran, S. S. Ramkumar** Electrospinning of Nanofibers 2005
- Timothy H. Grafe, Kristine M. Graham,** Nanofiber Webs from Electrospinning 2003.
- Varesano A, Carletto R A and Mazzuchetti G,** 2009 *J. Mater.- Process. Technol.* 209 5178.
- Vince Beachley, Xuejun Wen,** Effect of electrospinning parameters on the nanofiber diameter and length 2009
- Whitesides GM, Grzybowski B.** Self-assembly at all scales. *Science* 2002;295:2418–21.
- WilkesGL.** Available from: [http://yywww.che.vt.edu/Wilkesy -electrospinningyelectrspinning.html](http://yywww.che.vt.edu/Wilkesy-electrospinningyelectrspinning.html). 2001.
- Yarin AL, Koombhongse S, Reneker DH.** Bending instability in electrospinning of nanofibers. *J Appl Phys* 2001;89:3018–26.
- Yoshiro Yokoyama, Shinya Hattori, Chiaki Yoshikawa, Yoshihiro Yasuda, Hiroyuki Koyama, Tsuyoshi Takato, Hisatoshi Kobayashi** 2009.
- Z. M. Huang, Y. Z. Zhang, M. Kotaki, S. Ramakrishna,** *Compos.Sci. Technol.* 2003, 63, 2223.

**Zheng-Ming Huang, Y.-Z. Zhang, M. Kotaki, S. Ramakrishna**, A review on polymer nanofibers by electrospinning and their applications in nanocomposites, 2003.

## CURRICULUM VITAE



**Name Surname: Sassan JAHANGIRI**

**Place and Date of Birth: Tehran/Iran 21.09.1983**

**Address: N30, D13, Huzur Apt, SairNazim street, Muradiye district, Besiktash, Istanbul, Turkey.**

**E-Mail: [sassan.jahangiri@itu.edu.tr](mailto:sassan.jahangiri@itu.edu.tr) , [sassan.jahangiri@gmail.com](mailto:sassan.jahangiri@gmail.com)**

**B.Sc.: Textile Engineering**

**Professional Experience and Rewards:**

**2 Years of experiments in mineral chemistry analysis laboratory  
(Pajouheshgaran shimi Company) Iran/Tehran.**

**List of Publications and Patents:**

- H. Karakas, A.S. Saraç, **S. Jahangiri**, T. Polat, E.G. Budak, S. Bayram, N. Dağ, F. Kalaoğlu: Effect Of Electrospinning Process Parameters On The Production Of Polyurethane Nanofibers. 5<sup>th</sup> International Technical Congress, 7-9 November, 2012, Izmir, Turkey.
- H. Karakas, A.S. Sarac, T. Polat, E.G. Budak, S. Bayram, N. Dag, and **S. Jahangiri**: P-OLYURETHANE NANOFIBERS OBTAINED BY ELECTROSPINNING PROCESS. World Academy of science, Engineering and Technology, Vol:75 2013-03-23

## **PUBLICATIONS/PRESENTATIONS ON THE THESIS**

- H. Karakas, A.S. Sarac, T. Polat, E.G. Budak, S. Bayram, N. Dag, and **S. Jahangiri**: POLYURETHANE NANOFIBERS OBTAINED BY ELECTROSPINNING PROCESS. World Academy of science, Engineering and Technology, Vol:75 2013-03-23
- H. Karakas, A.S. Saraç, **S. Jahangiri**, T. Polat, E.G. Budak, S. Bayram, N. Dağ, F. Kalaoğlu: Effect Of Electrospinning Process Parameters On The Production Of Polyurethane Nanofibers. 5th International Technical Congress, 7-9 November, 2012, Izmir, Turkey.